University of Kentucky
UKnowledge

Theses and Dissertations--Mechanical Engineering | Mechanical Engineering

2016

Diffusion-Mediated Deposition of Proteins

Ruiqian Zhan
University of Kentucky, rzh238@g.uky.edu
Digital Object Identifier: http://dx.doi.org/10.13023/ETD.2016.358

Click here to let us know how access to this document benefits you.

Recommended Citation

Zhan, Ruiqian, "Diffusion-Mediated Deposition of Proteins" (2016). *Theses and Dissertations--Mechanical Engineering*. 81.
https://uknowledge.uky.edu/me_etds/81

This Master's Thesis is brought to you for free and open access by the Mechanical Engineering at UKnowledge. It has been accepted for inclusion in Theses and Dissertations--Mechanical Engineering by an authorized administrator of UKnowledge. For more information, please contact UKnowledge@lsv.uky.edu.

STUDENT AGREEMENT:

I represent that my thesis or dissertation and abstract are my original work. Proper attribution has been given to all outside sources. I understand that I am solely responsible for obtaining any needed copyright permissions. I have obtained needed written permission statement(s) from the owner(s) of each third-party copyrighted matter to be included in my work, allowing electronic distribution (if such use is not permitted by the fair use doctrine) which will be submitted to UKnowledge as Additional File.

I hereby grant to The University of Kentucky and its agents the irrevocable, non-exclusive, and royalty-free license to archive and make accessible my work in whole or in part in all forms of media, now or hereafter known. I agree that the document mentioned above may be made available immediately for worldwide access unless an embargo applies.

I retain all other ownership rights to the copyright of my work. I also retain the right to use in future works (such as articles or books) all or part of my work. I understand that I am free to register the copyright to my work.

REVIEW, APPROVAL AND ACCEPTANCE

The document mentioned above has been reviewed and accepted by the student's advisor, on behalf of the advisory committee, and by the Director of Graduate Studies (DGS), on behalf of the program; we verify that this is the final, approved version of the student's thesis including all changes required by the advisory committee. The undersigned agree to abide by the statements above.

Ruiqian Zhan, Student

Dr. Christine Ann Trinkle, Major Professor

Dr. Haluk Karaca, Director of Graduate Studies

DIFFUSION-MEDIATED DEPOSITION OF PROTEINS

THESIS

A thesis submitted in partial fulfillment of the
requirements for the degree of Master of Science in
Mechanical Engineering in the College of Engineering
at the University of Kentucky

By

Ruiqian Zhan

Lexington, Kentucky

Director: Dr. Christine Ann Trinkle, Professor of Mechanical Engineering

Copyright © Ruiqian Zhan 2016

ABSTRACT OF THESIS

DIFFUSION-MEDIATED DEPOSITION OF PROTEINS

Gradients of proteins play a prominent role in many biological processes, from development of multicellular organisms to chemical signaling in the immune system. Deposition of surface gradients is a way to permanently modifying a surface's properties, resulting in the creation of novel materials which have widespread applications in biologically relevant fields, such as directed cell growth, production of biocompatible implantable materials, and creation of functional biosensors. These types of surfaces can also be used as an *ex vivo* tool to help understand many biological processes by mimicking the environment in gradient-related phenomena in a controllable way. However, despite the large number of applications for chemically graded surfaces, creating them remains a challenge.

In this work, a novel diffusion-based patterning mechanism is presented that relies on a 3D micropatterned poly(ethylene glycol) diacrylate (PEG) 'stamps' for the controlled deposition of fluorescently-tagged protein 'ink' onto pre-treated glass slides. By controlling the contact time and mechanical deformation of the PEG hydrogel on the glass surfaces, it is possible to control local concentration of protein deposition.

KEYWORDS: Protein Deposition, Surface Patterning, Gradients, Hindered Diffusion, 3D Microfabrication

Ruiqian Zhan

Student's Signature

July 28, 2016

Date

DIFFUSION-MEDIATED DEPOSITION OF PROTEINS

By

Ruiqian Zhan

Christine Ann Trinkle

Director of Thesis

Dr. Haluk Karaca

Director of Graduate Studies

July 28, 2016

Date

ACKNOWLEGEMENT

I would like to express my sincere gratitude to my advisor, Dr. Christine A. Trinkle, for her support, guidance, and motivation as well as encouragement. She opened the doors to Deposition of Protein for me. She deserves a tremendous amount of credit for this work and my development as a researcher and technical writer. I would also like thank Dr. Sean Bailey and Dr. L. Scott Stephens for being my thesis committee members and critical review of my work.

I would like to thank my labmates, Ning Ge and Soroosh Torabi, for their sharing hands-on experience, scientific discussions, suggestions and advices on my research. They make my study and research experience in the lab pleasant and memorable.

I would love to thank my family for their unconditional love, support and encouragement. Without their support for whether economy or psychology, I cannot finish my master degree.

Last, this material is based upon work supported by the National Science Foundation under Grant No. CMMI-1125722.

TABLE OF CONTENTS

ACKNOWLEGEMENT iii
TABLE OF CONTENTS iv
LIST OF TABLE v
LIST OF FIGURES vi
Chapter 1 Introduction 1
1.1 Background and Motivation 1
1.2 Thesis Organization 2
Chapter 2 Literature Review 5
2.1 Surface Patterning of Chemicals and Proteins 5
2.2 Surface Gradient Generation of Proteins 13
Chapter 3 Theoretical Background 21
3.1 Relationship between Deformation of PEG and Contact Area 21
3.2 Solute Diffusion within Hydrogels 26
Chapter 4 Experimental Device Design 30
4.1 Microcontact Printing System 30
Chapter 5 Protein Printing 34
5.1 Creation of Hemispherical PEG Hydrogel Stamp using PDMS Mold 34
5.1.1 Creation of PDMS Mold 34
5.1.2 Fabrication of Hemispherical PEG Hydrogel Stamp 36
5.2 Preparation of Target Surface 38
5.3 Uniform-Concentration Protein Printing 39
5.4 Multi-step Protein Printing 43
Chapter 6 Conclusions and Future Work 46
6.1 Conclusions 46
6.2 Future Work 47
References 48
Vita 52

LIST OF TABLE

Table 1 Fluorescent intensity profile. 43

LIST OF FIGURES

Figure 1 Microcontact printing of proteins from hydrogel onto treated surface by using time-varying contact pressure and local polymer stamp deformation to control contact time and solute transfer.....2
Figure 2 (A) Schematic description for the fabrication of Au patterns using PDMS, (B) SE micrographs of features produced through multiple stamping [1]. 5
Figure 3 (a) Printing isolated features using conventional thick stamp μCP. Stamp sagging causes printing in undesired locations. (b) Printing isolated features using a thin stamp with a rigid back support; stamp sagging is eliminated [3]. 7
Figure 4 (A) General scheme for antibody "stamping" followed by exposure to labeled antigen. IgG orientation is idealized. (B) Sequential visualization of three different antigens bound to stamp IgGs [5]. 8
Figure 5 (A) Patterned elastomer that forms a μFN by contact with a substrate allows the local delivery of a solution of biomolecules to the substrate, (B) Flow of liquid between the filling pad and an opposite pad fills the array of microchannels, (C) Pattern of chicken IgG on gold [10].....9
Figure 6 Sixteen different proteins (some of them without fluorescent label) were patterned onto the polystyrene surface of a cell culture dish using a stamp inked by means of a microfluidic network [11]. 10
Figure 7 Scheme for the fabrication of 3D-microfluidic stamp [13]. 11
Figure 8 3D-microfluidic networks patterning. (A)and (C)shows flow patterns in 3D stamp, (B) The bright green spiral is BSA; the light green one is fibrinogen, (D) The differences in the thickness of the SiO_2 layer gave rise to the different interference colors in the etched pattern. These colors are caused by interference between light reflected from the air/SiO2 interface and that from the Si/SiO_2 interface; they reveal the depth of etching [13]. 12
Figure 9 (A) Schematic of the BioLP apparatus as it pertains to printing protein microarrays. (B) BioLP printed drops of BSA solution [17]. 13
Figure 10 (A) Fluorescence-labeled mouse-IgG was deposited on Si_3N_4 and exposed to different light exposure [24]. 14
Figure 11 Continuous gradients of antigens (rabbit IgGs) were produced by a μFN on a PDMS surface [9]. 15
Figure 12 Schematic of the channel outgas filling process and formation of protein gradient [25].....16
Figure 13 (a) Multiple-gradient array of BSA-TRITC formed in 70-μm channel width device. (b) Counterpropagating gradient of BSA-TRITC (red) and collagen-Oregon Green (green) [25]. 16

Figure 14 Schematic drawing of the design of a typical microfluidic network in to PDMS used for the fabrication of immobilized gradient [27]. 17
Figure 15 Overlapping gradients of two fluorescently labeled proteins on an aldehyde-functionalized glass slide. (A) A gradient with a high surface concentration of FITC-BSA on the left and a low surface concentration of FITC-BSA on the right side. (B) A gradient with a high concentration of TRITC-BSA at the right side of the image and a low concentration of TRITC-BSA at the left side on the same position of A [28]. 18
Figure 16 Electrospinning of nanofibers and deposition of protein gradient. (A) polymer fibers were deposited on an ITO glass slide; (B) peotein gradient was generated on the fiber layer by speed controlled filling; (C) scanning electronic micrography of randomly deposited PMGI fibers; (D) fluorescent micrograph of the slide after filling with a solution of FITC-labeled fibronectin for a total length of about 10 mm; (E) corresponding fluorescence intensity profile of the fiber-coated slide [29]. 19
Figure 17 Deformation of hydrogel hemisphere and microscope images of contact circles for low and high pressure cases. 22
Figure 18 Relationship between distance from hydrogel base to surface (h), contact radius (r), and hemisphere diameter (d). 24
Figure 19 Magnitude of the stress components below the surface as a function of the maximum pressure of contacting sphere. 25
Figure 20 Model of blind-well chambers; from [42] 28
Figure 21 Drawing of assembled microcontact printing system. 30
Figure 22 Base printing platform that attached to the microscope stage, all dimensions in millimeters 31
Figure 23 Precision z-stage (Dimensioned drawing provided by manufacturer), all dimensions in millimeters. 32
Figure 24 Hydrogel stamp platform; all dimensions in millimeters. 33
Figure 25 (A) Metal spheres with different diameters used for making the initial mold cavity. (B) One of the laser-cut acrylic pieces. (C) PDMS mold. (D) Hemispherical PEG. 34
Figure 26 Preparation of PDMS hemispherical mold. 35
Figure 27 Preparation of Hemispherical PEG Hydrogel Stamp. 37
Figure 28 Schematic of glass surface functionalization and fluorescent tagged protein attachment. 38
Figure 29 Fluorescent image resulting from single-step printing of hydrogel for 5 minutes. 41
Figure 30 Normalized fluorescent intensity versus contact time. 42

Figure 31 Dual pressure protein printing. 44
Figure 32 Multiple pressure protein printing. Contact time from outer to inner are 30s, 2 min, 8min, and 20 min.....44

Chapter 1 Introduction

1.1 Background and Motivation

Gradients of proteins play a prominent role in many biological processes, from development of multicellular organisms to chemical signaling in the immune system. Deposition of surface gradients is a way to permanently modifying a surface's properties, resulting in the creation of novel materials which have widespread applications in biologically relevant fields, such as directed cell growth, production of biocompatible implantable materials, and creation of functional biosensors. These types of surfaces can also be used as an *ex vivo* tool to help understand many biological processes by mimicking the environment in gradient-related phenomena in a controllable way. However, despite the large number of applications for chemically graded surfaces, creating them remains a challenge.

In this work, a novel diffusion-based patterning mechanism is presented that relies on a 3D micropatterned poly(ethylene glycol) diacrylate (PEG) 'stamps' for the controlled deposition of fluorescently-tagged protein 'ink' onto pre-treated glass slides (Figure 1). By controlling the contact time and mechanical deformation of the PEG hydrogel on the glass surfaces, it is possible to control local concentration of protein deposition. Experimental results show that this method can be used to generate micropatterns with uniform density of proteins on pre-treated surface. Additionally, intentionally "stepped" micropatterns with regions of different protein density can be printed by controlling contact pressure and time between the PEG

and the target surface. Using these results, careful design of hydrogel topography, and precise control of contact pressure, it may be possible to extend this method in the future to print gray-scale surface patterns of virtually any concentration.

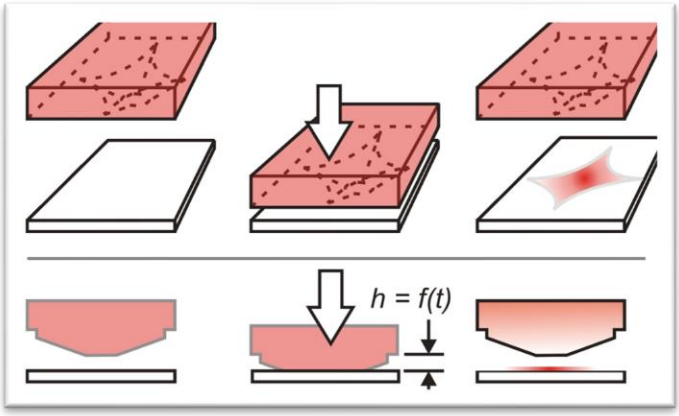

Figure 1 Microcontact printing of proteins from hydrogel onto treated surface by using time-varying contact pressure and local polymer stamp deformation to control contact time and solute transfer

1.2 Thesis Organization

The research presented in this thesis involves surface patterning of proteins using 3D micropatterned PEG. Proteins can diffuse through the mesh microstructure created by the cross-linked polymer chains within the PEG hydrogel. When a PEG hydrogel that contains a uniform concentration of a protein is brought into contact with a target surface, the protein will absorb onto the surface, locally depleting the protein concentration within the PEG. These molecules will be replenished as proteins diffuse from the body of the PEG to the surface. By controlling the density of cross-linking within the hydrogel, the size of proteins in the hydrogel, and the volume fraction of water within the PEG, the diffusion rate of the protein can be adjusted.

In this research, a novel microprinting mechanism was developed based on this method of molecular transport within hydrogels, combined with local deformation of compliant hydrogel hemispheres. 3D PEG “stamps” were installed on a height changeable printing platform, which was used to bring the PEG into controlled contact with microscope cover glass that was chemically pretreated so that it would bind the protein molecules that came into contact with it. A fluorescently-tagged protein was used as the “ink” inside the PEG stamp, making it possible to use fluorescent intensity to determine the relative concentration of proteins deposited on the surface. By controlling the amount of time the hydrogel was in contact with the target glass surface, it was possible to locally control protein deposition.

This thesis consists of 6 chapters with the following content:

- Chapter 1 provides a brief introduction to the thesis and the research presented herein.
- Chapter 2 reviews past and current research work in the field of surface patterning of chemicals and proteins, with a special emphasis on the creation of surface gradients of chemicals and proteins.
- Chapter 3 explains two fundamental physical mechanisms used in this microcontact printing method: deformation in Hertzian contact and hindered diffusion of molecules in hydrogels.

- Chapter 4 discusses the design and components of the microcontact printing device and how the device functioned once assembled.
- Chapter 5 illustrates the creation of hemispherical PEG hydrogel stamps and using these hydrogels to create protein surfaces with uniform concentration, binary concentrations, and multiple concentration steps.
- Chapter 6 summarizes the work presented in this thesis and discusses possible future work on this project.

Chapter 2 Literature Review

2.1 Surface Patterning of Chemicals and Proteins

Modifying a surface with biomolecules such as proteins or DNA has wide-reaching applications among many biologically-related fields: medical diagnostics, culturing cells, or synthesizing carbohydrates, polypeptides and DNA to name a few. Proteins cannot be easily synthesized on a solid surface, but can be transferred to a target surface using a number of patterning or printing methods. One of the most widely used method for patterning of proteins is micro-contact printing (μCP), shown in Figure 2. This method was originally developed by Whitesides and coworkers at Harvard in 1993 [1].

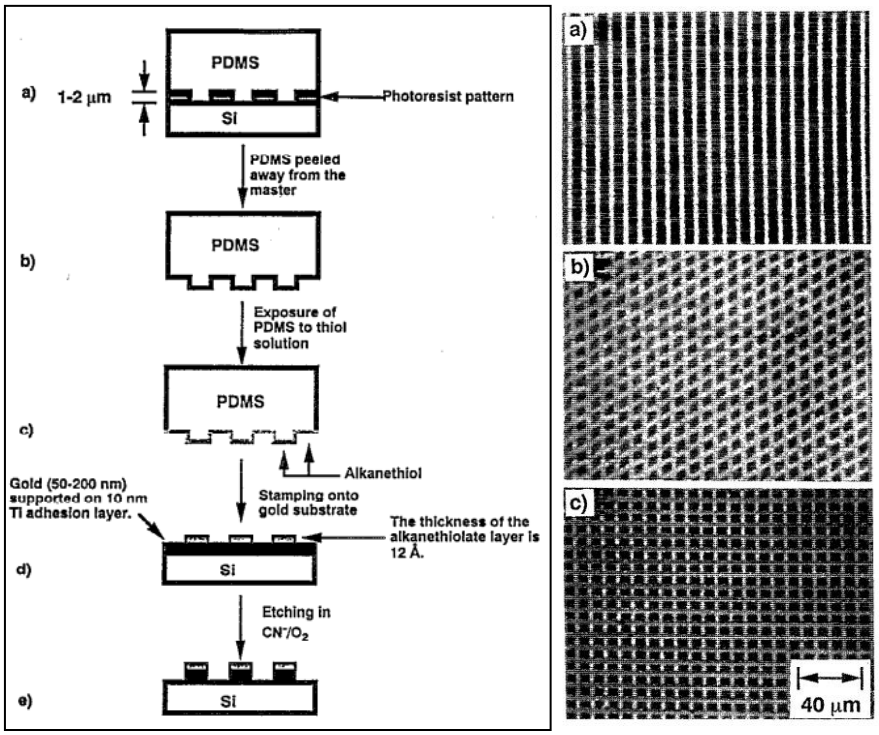

A B

Figure 2 (A) Schematic description for the fabrication of gold patterns using PDMS microcontact printing, (B) SEM images of features produced with multiple stamping steps [1].

The Whitesides group used polydimethylsiloxane (PDMS) stamps with micropatterned surface features, which they exposed to a solution of alkanethiol "ink." The alkanethiols adsorbed onto the PDMS surface, so that when dried, these stamps could be used to transfer self-assembled monolayers (SAMs) of the alkanethiol onto a gold surface. In this work, they followed this step with an etching processes in an aqueous solution to obtain patterned gold features ranging in scale from micrometers to centimeters.

Bernard and co-workers extended this method to create micropatterns of proteins using μCP [2]. Featured PDMS stamps were incubated with protein solutions and then dried; the protein retained on the PDMS could be transferred to a target surface with only ~1 second of contact between the two. The advantage of this method is that the average density of proteins in the patterned area printed onto the surface could be controlled by adjusting the concentration of protein solution during inking process. However, each region of the stamp that contacts the target surface will transfer the same protein density, meaning that the overall effect is a "binary" pattern.

James and co-workers further improved previous micro-contact printing methods [3]. They overcame two major problems with early μCP: one was difficulty in printing water-based biological solutions (such as proteins in saline solution) because the PMDS stamp used in μCP was hydrophobic, the other issue was a lack of precision in

alignment and patterning caused by the very compliant material of the soft elastomer stamps. They solved the first problem by exposing PDMS to a low temperature plasma, causing the surface to become hydrophilic. The second problem was solved by fabricating thin elastomer stamps on a stiff glass backing to eliminate sagging and handling problems experienced in conventional thick stamp printing (Figure 3).

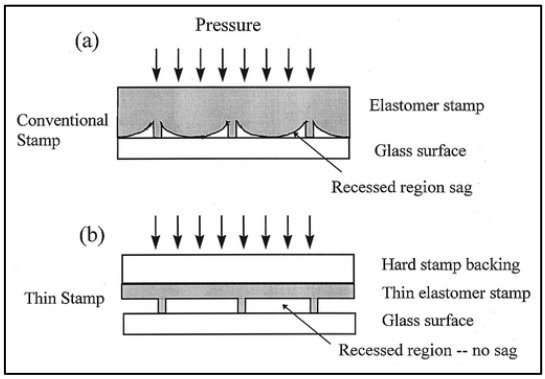

Figure 3 (a) Printing isolated features using conventional µCP; stamp sagging causes pattern transfer in undesired locations. (b) Printing isolated features using a thin stamp with a rigid back support; stamp sagging is eliminated [3].

Patel and co-workers further improved microcontact printing of proteins by using a high-affinity bond to immobilize printed protein on the surface [4]. Prior microcontact printing relied on the non-covalent absorption of protein onto the surface, which resulted in reversible attachment. In contrast, Patel exploited high affinity avidin-biotin receptor-ligand interactions by coating a substrate with biotin molecules and then microcontact printing avidin micropatterns onto the surface. This surface chemistry was also used in the patterning experiments in this thesis.

While the majority of microcontact printing work utilized PDMS as the stamp material, Martin and co-workers instead used cross-linked poly-(6-acryloyl-β-O-methyl-galactopyranoside) as stamps [5]. They created this cross-linked hydrogel in the narrow ends of machine-pulled capillary tubes and loaded them with protein solution. Then the hydrogel/capillary stamp was brought into contact with an aminosilylated target surface for approximately 2 seconds, followed by raising stamp, shifting substrate and printing again until desired patterns were formed (Figure 4).

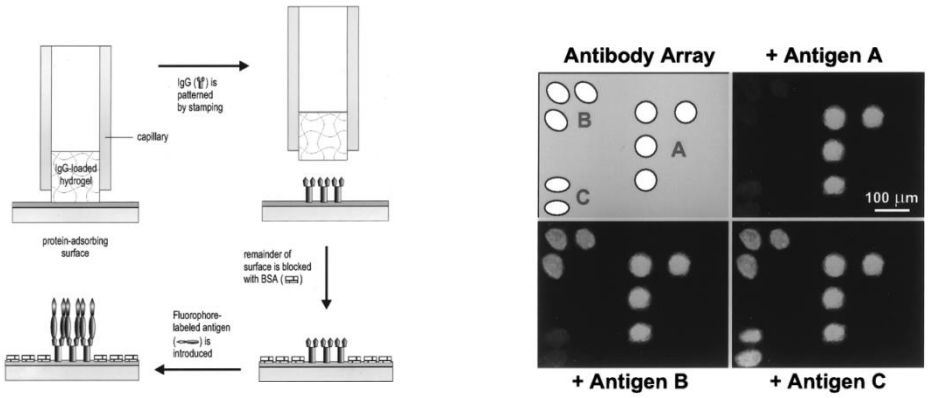

A B

Figure 4 (A) Method for antibody hydrogel "stamping" followed by exposure to labeled antigen. (B) Sequential visualization of three different antigens bound to stamped IgGs [5].

Microcontact printing and its numerous variations have gained widespread use because of its simplicity and ability to create high resolution micropatterns. However, it is generally difficult to use this method to create patterns containing multiple, aligned patterns of different proteins on the same surface. Microfluidic printing is one popular method that has overcome this hurdle. In this method, networks of

microfluidic channels can be used to create microarrays of biological molecules [6][7] by guiding liquid solutions of biochemicals over contact areas with substrates, as shown in Figure 5. Using this method, it is possible to localize the absorption of proteins to the regions in contact with the channels. After the patterning is complete, the channel is dried and the microfluidic channel network can be peeled off of the surface, leaving behind only the patterns of biochemical adsorbed on the surface.

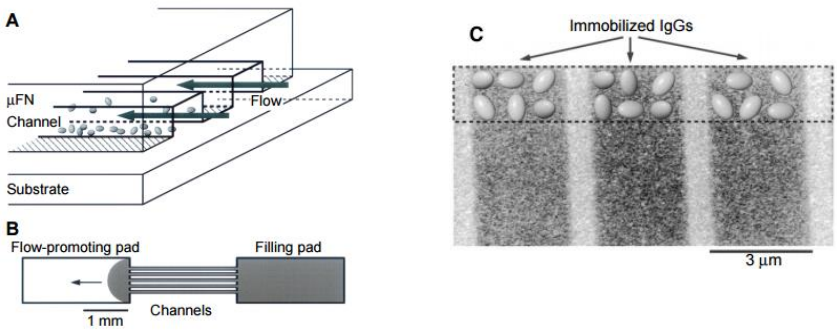

Figure 5 (A) Patterned elastomer that forms a μFN by temporarily attaching it to the surface of a substrate, allowing local delivery of a solution of biomolecules to the substrate, (B) Flow of liquid between the filling pad and an opposite pad draws liquid into the array of microchannels, (C) Pattern of chicken IgG on gold [6].

Using microfluidic patterning, it is possible to make controllable, high resolution surface patterns. However, there are several requirements for successful protein transfer using this method [6][8][9]: the material of the microfluidic networks (μFNs) must be sufficiently hydrophobic, the contact area between μFNs and substrates should be sealed well, the μFN should be capable of promoting the flow of a large volume of solution, and the surfaces of μFNs should resist protein absorption in order to prevent undesired protein loss.

Bernard A. and co-workers used microfluidic networks as a strategy for parallel printing of multiple proteins [10], as shown in Figure 6. They fabricated a microfluidic network with 16 microchannels which contained 16 different proteins, then transferred them from flat stamp to a plastic substrate. By using this method, they were able to print multiple proteins at once with precise alignment between the patterns and without using the complex and difficult process of using multiple-stamp microcontact printing.

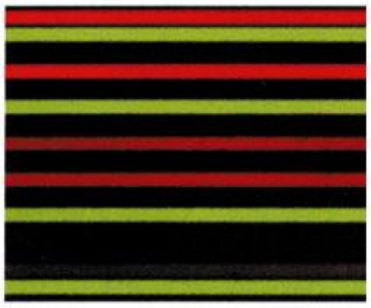

Figure 6 Sixteen different proteins (some of them without fluorescent labels) were patterned onto the polystyrene surface of a cell culture dish using a stamp inked by means of a microfluidic network [10].

Other researchers have extended this basic microfluidic patterning concept. Papra and co-workers coated series type of µFN-made of PDMS, Si and Au-with Polyethylene Glycol making them hydrophilic enough for driving protein solution self-filling by capillary force and ideally resist the absorption of proteins [11]. Chiu and co-workers [12] used a 3D micromolding in capillaries (MIMIC) technique that they developed [7][13][14][15] to fabricate 3D µFNs for patterning complex and discontinuous multiple proteins or cells on planar surfaces.

There are five major steps for making a 3D-microfluidic network, as shown in Figure 7: (i) fabrication of silicon master for the top PDMS slab, (ii) fabrication of a photoresist-patterned silicon master for the bottom of the PDMS membrane, (iii) creating the PDMS slab that forms the top layer of the device using silicone master fabricated in step (i), (iv) creating a PDMS membrane which will form the bottom layer of the device using silicone master fabricated in step (ii), and (v) assembling and sealing top and bottom layers of PDMS with a substrate.

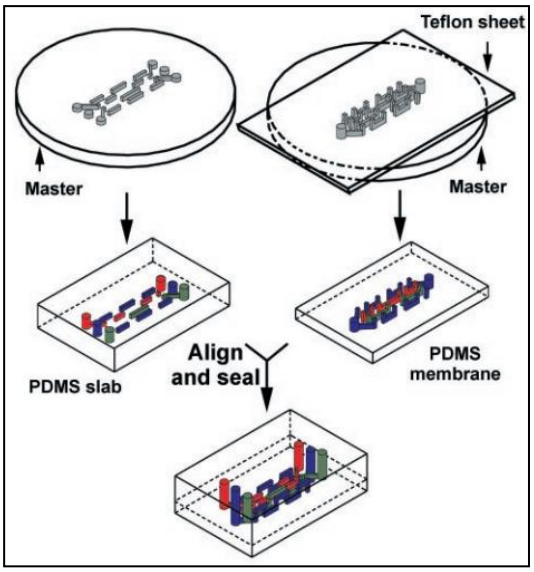

Figure 7 Method for the fabrication of 3D-microfluidic networks [12].

Using these 3D microfluidic networks, Chiu et al successfully etched Si/SiO_2 wafer substrates to three different depths using three different concentrations of HF (Figure 8 C and D) and also used this method to patterned two kinds of proteins in a nested spiral (Figure 8 A and B).

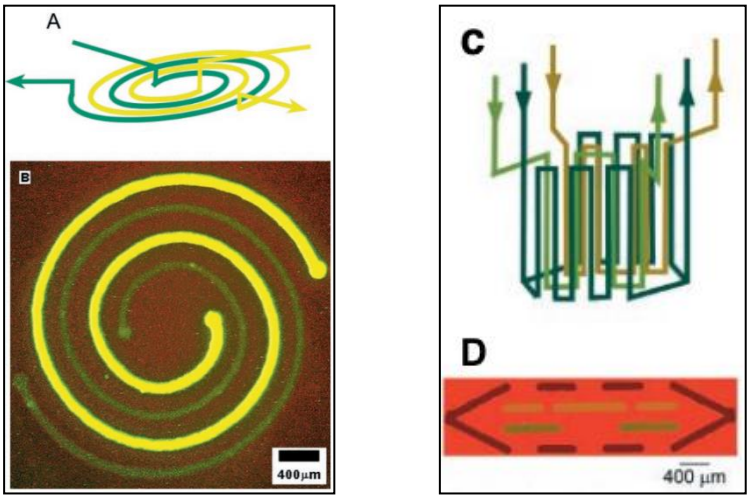

Figure 8 3D-microfluidic network patterning. (A)and (C)shows flow patterns in the 3D stamp, (B) The bright green spiral is BSA; the light green one is fibrinogen, (D) The differences in the thickness of the SiO_2 layer gave rise to the different interference colors in the etched pattern. These colors are caused by interference between light reflected from the air/SiO2 interface and that from the Si/SiO_2 interface; they reveal the depth of etching [12].

There are a wealth of other, non-contact methods of depositing patterns of biological molecules. One of the more unique methods is biological laser printing (BioLP) which can be used for creating protein microarrays [16]. It is a capillary-free printing method that overcomes clogging problems among conventional solid pin printing instruments used for cDNA microarray fabrication [17][18][19]and can create protein microarrays on a variety of surfaces and with droplets scaling from femtoliter to nanoliter [20][21]. Using this method, it is possible to get highly controlled protein volume and position deposited from solution (Figure 9). Droplets are ejected from solution on the target support towards the receiving substrate due to heat transfer caused by laser absorption at the laser absorption interlayer. By controlling laser fluence, it is possible to change the fluid ejection volume.

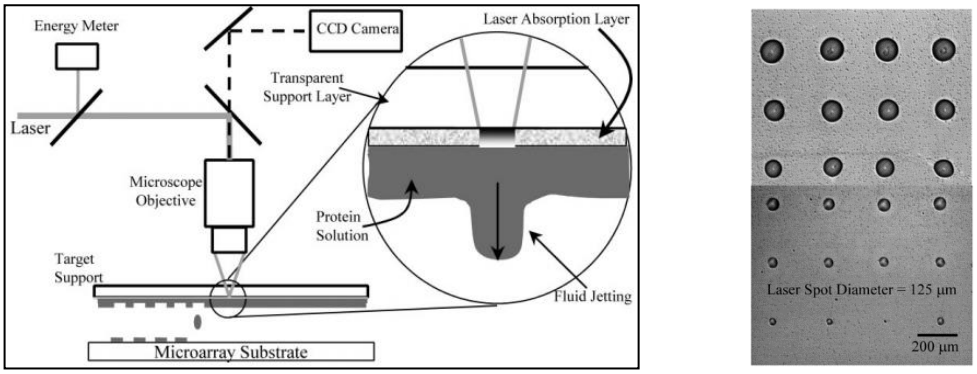

A B

Figure 9 (A) Schematic of the BioLP apparatus as it pertains to printing protein microarrays. (B) BioLP printed drops of BSA solution [16].

2.2 Surface Gradient Generation of Proteins

The body of research described in the previous section focuses on binary deposition of molecules onto a target surface. However, the goal of the research presented in this thesis is to eventually be able to deposit surfaces with controllable local molecule concentration (i.e., “gray-scale” surfaces).

Hypolite and co-workers synthesized photoactivatable molecules with fluorescent proteins and immobilized them in a gradient pattern on a polystyrene surface by controlling laser-scanning speed [21]. In this method, protein was mixed with photolinker polymer which can generate reactive carbenes when exposed to light. These carbenes can bind with adjacent surface materials or biomolecules, thus irreversible links between proteins and the surface could be generated. By controlling laser-scanning speed and position, it is possible to generate complex gradient protein patterns. Isabelle Caelen and co-workers [22] also used photosensitive molecules

which can bind with surface materials and proteins. They mixed a photosensitive polysaccharide-based polymer with proteins and spotted them onto Si_3N_4 chips using an ink-jet printer. By exposing chips to light for different durations, they were able to generate different surface concentrations of protein (Figure 10). However, these methods both require complex chemical synthesis and are not compatible with all types of biochemicals.

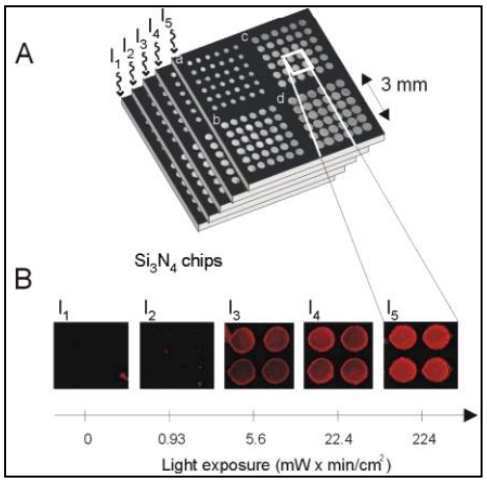

Figure 10 (A) Fluorescent-labeled mouse IgG was deposited on Si_3N_4 and exposed to different light exposure times to create different surface concentrations [22].

Caelen and co-workers used a modified version of microfluidic patterning to create gradients of protein on a target surface [23]. They fabricated long microchannels on a silicon wafer and sealed it with a PDMS substrate. Because of the length of the channels and fast absorption of proteins into the surface of PDMS, it depleted the protein concentration in solution along the length of the channel, creating a gradient as shown in Figure 11.

Figure 11 Continuous gradients of protein (rabbit IgG) produced using high aspect ratio μFNs on a PDMS surface [23].

Fosser and Nuzzo used fluid flow into a PDMS microfluidic network to generate linear protein gradients in a single microchannel, and even demonstrated two opposing protein gradients from opposite directions of a microchannel [24]. They applied a channel outgassing technique [25] to fill the channel using negative pressure rather than positive pressure in order to overcome bubble generation and other filling problems that often appear in traditional microfluidic filling processes. In this method, covered the inlet of a microchannel with a protein solution and sealed the channel outlet using a glass piece. Then the whole device was put into a vacuum chamber, and the time and pressure were controlled over a period of time to slowly control the rate of filling, as shown in Figure 12. Using this method, it is possible to generate multiple gradients of a single protein on a surface (Figure 13a), or by using a reverse-filling technique, to generate multiple patterns of two different proteins (Figure 13b).

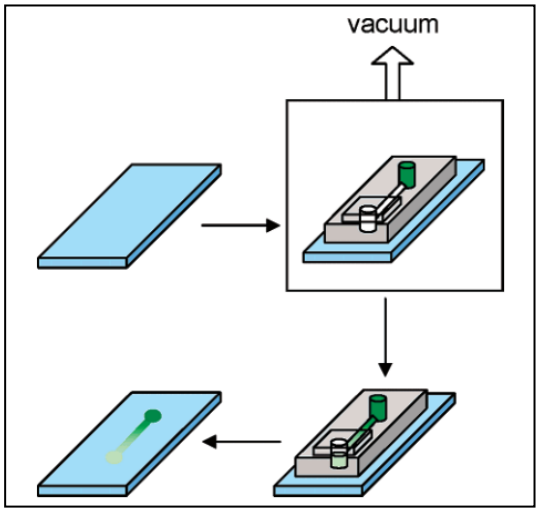

Figure 12 Schematic of the microfluidic channel outgas filling process to form a protein surface gradient [24].

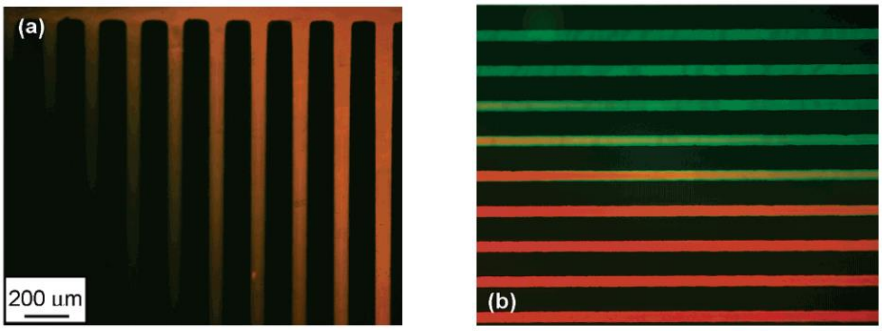

Figure 13 (a) Multiple-gradient array of BSA-TRITC formed in a 70-µm channel width device. (b) Counterpropagating gradient of BSA-TRITC (red) and collagen-Oregon Green (green) [24].

Whitesides and co-workers [26] generated controllable protein gradients by using microfluidic networks that split and recombined two initial inlet streams to eventually form 5 individual channels each with unique protein solution concentration. These channels then merged into a single wide channel to produce laminar flow of protein solution, creating protein gradients (Figure 14). By controlling the solution concentration in the input channels, the design of the microfluidic

network, they were able to control the shape of gradients much better than previous microfluidic gradient patterning methods.

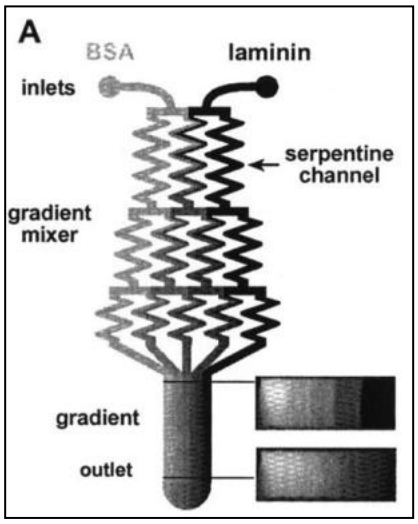

Figure 14 Schematic drawing of a typical microfluidic network in PDMS used for patterning of immobilized surface protein gradient [26].

Mayer and co-workers used diffusion within a hydrogel to pattern a gradient of two counterpropagating fluorescent-tagged proteins on a flat surface [27]. To do this, they cured agarose solution onto a Si wafer to get a strip of agarose with a flat surface. They then sealed the flat surface of the agarose with a PDMS strip and introduced fluorescently tagged proteins (FITC-BSA and TRITC-BSA) to either of the two sides of the agarose strip. After proteins diffused from the ends into the gel setting up a gradient of proteins within the agarose, the PDMS strip was removed and glass slide functionalized with aldehyde groups was applied. The protein gradient transferred successfully to the glass slide (Figure 15). There are several advantages to

this method: (i) it can transfer two protein gradients at once, (ii) it can generate multiple arrays of proteins with small quantities of protein, (iii) it can absorb excess solution during inking, and (iv) because the proteins stay in solution during the gradient generation process, the hydrogel provides a good environment for protein stability.

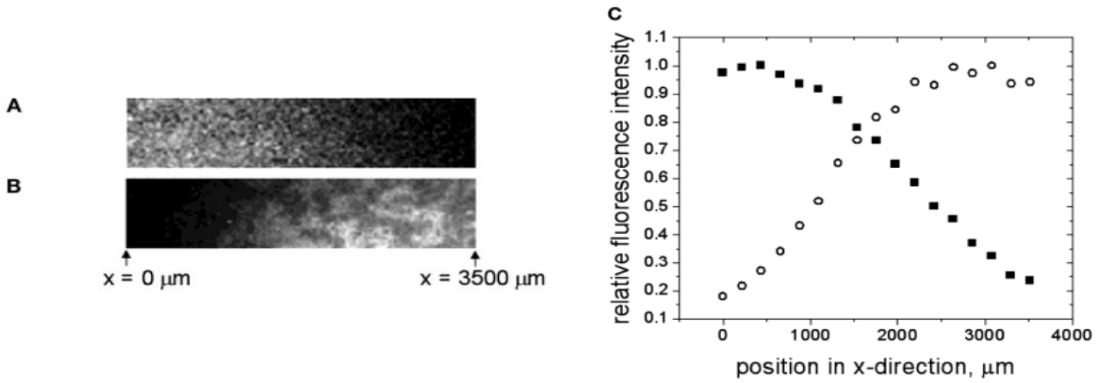

Figure 15 Overlapping gradients of two fluorescently labeled proteins on an aldehyde-functionalized glass slide. (A) A gradient with a high surface concentration of FITC-BSA on the left and a low surface concentration of FITC-BSA on the right side. (B) A gradient with a high concentration of TRITC-BSA at the right side of the image and a low concentration of TRITC-BSA at the left side on the same position of A [27].

Jian Shi and co-workers used controlled submersion of a substrate into a protein solution to generate a surface gradient [28]. They built a PDMS chamber and put a fiber-coated substrate into the chamber; by controlling the speed of input of solution from the bottom of the chamber, they were able to control the amount of time a region spent immersed in protein solution, creating a gradient of protein deposited on the fiber-coated substrate (Figure 16).

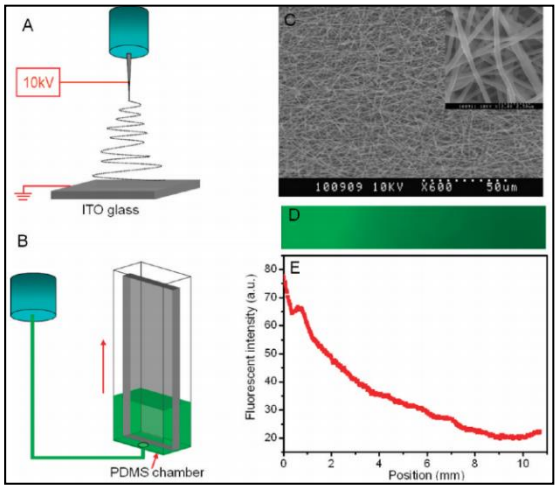

Figure 16 Electrospinning of nanofibers and deposition of protein surface gradient. (A) polymer fibers were deposited on an ITO glass slide; (B) protein surface gradient was generated on the fiber layer by controlled filling of a chamber; (C) scanning electronic micrograph of randomly deposited electrospun fibers; (D) fluorescent micrograph of the slide after filling with a solution of FITC-labeled fibronectin for a total length of about 10 mm; (E) corresponding fluorescence intensity profile of the fiber-coated slide [28].

Krämer and co-workers [29] also applied this controlled-filling method, but employed colloidal metal nanoparticles as protein carriers to form protein gradients. In general, this method does not require expensive or sophisticated equipment and has been demonstrated with many compatible molecules, such as thiols [30][31] and alkylsilanes [32][33][34][35]. These chemical modifications can be used to control protein deposition on a surface, so it is also indirectly applicable for protein surface patterning.

Vasilev and co-workers [36] grafted a gradient of PEG molecules onto a surface; these molecules are known to resist protein absorption when deposited with sufficient density onto a solid surface [37]. This method was then used indirectly for the deposition of large and small proteins in surface gradients. The large protein was

incubated at the low PEG density side first and then the small protein was absorbed between the high PEG density and large protein.

It is important to note that the microfluidic gradient patterning methods described here can only be used to produce relatively simple gradients: constantly increasing or decreasing in density along a single direction. So while it is possible to locally control the protein deposition concentration to an extent, it is impossible to use these methods for true gray-scale printing.

Chapter 3 Theoretical Background

This chapter focuses on describing the physical mechanisms behind the diffusion-based microcontact printing method presented in this thesis. This method relies on elastic deformation of a three-dimensional hydrogel stamp and the diffusion of proteins through the hydrogel to generate complex surface patterns. The elastic deformation can be modeled using Hertzian contact theory, which can be used to predict the relationship between contact force and contact area. The motion of proteins through hydrogel can be estimated using a diffusion model. Both of these models will be discussed in this chapter.

3.1 Relationship between Deformation of PEG and Contact Area

Using Hertzian contact theory, it is possible to predict the behavior of two spheres of diameter d_1 and d_2 pressed together with a force F. This case would result in a circular contact area between the spheres, having a radius r:

$$r = \sqrt[3]{\frac{3F}{8}\frac{(1-v_1^2)/E_1 + (1-v_2^2)/E_2}{1/d_1 + 1/d_2}} \qquad 3.1$$

where E_1, v_1 and E_2, v_2 are the respective Elastic Modulus (E) and Poisson's ratio (v) of the materials of the two spheres.

In the case of interest here, we want to analyze a hydrogel hemisphere pressed against a flat glass surface. We assign the subscript 1 to the hydrogel (E_1, v_1, d_1)

and the subscript 2 to the glass surface (E_2, v_2, d_2). Because the glass surface is flat, it has an infinite diameter (d_2 = ∞), thus $1/d_2$ = 0. Also, because the elastic modulus of the hydrogel is much smaller than that of the glass ($E_1 \ll E_2$), the contribution of the $(1-v_2^2)/E_2$ term is negligible compared to the $(1-v_1^2)/E_1$ term. Therefore, we can approximate the radius r of contact area as:

$$r \approx \sqrt[3]{\frac{3F}{8}\frac{(1-{v_1}^2)d_1}{E_1}} \qquad 3.2$$

This indicates that higher contact force results in a larger contact area as shown in Figure 17; specifically, the radius scales as $r \sim F^{1/3}$

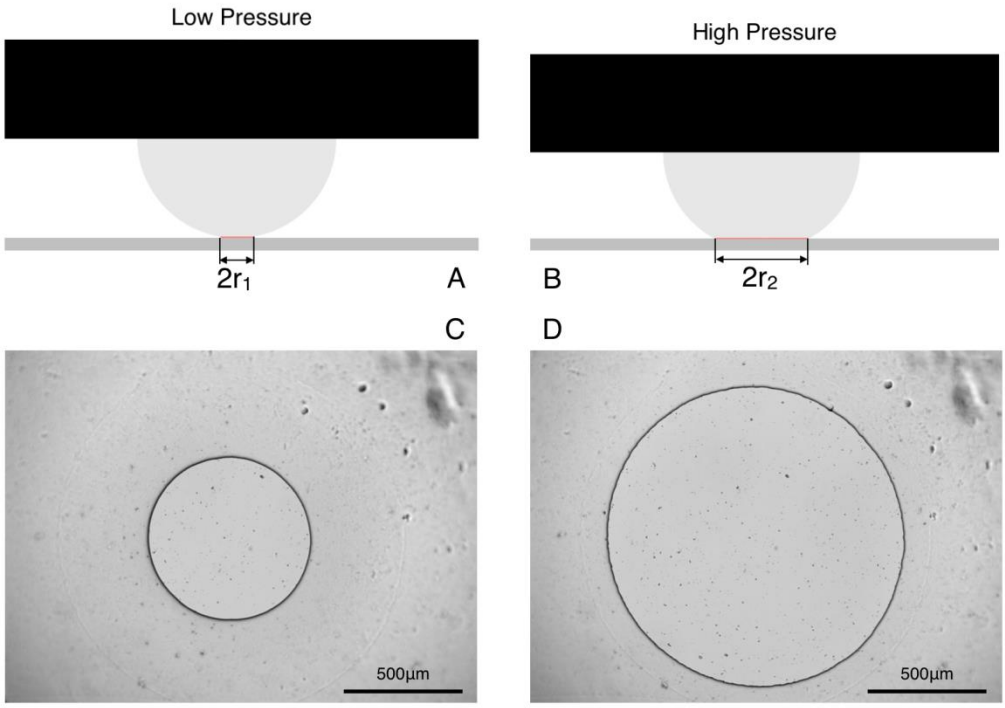

Figure 17 Deformation of hydrogel hemisphere and microscope images of contact circles for low and high pressure cases.

In order to determine the relationship between the vertical deformation of the stamp during contact and the contact radius, we define the Equivalent modulus of elasticity, E_e, to be a function of the material properties of the two materials [39]:

$$E_e = \left(\frac{1-v_1^2}{E_1} + \frac{1-v_2^2}{E_2}\right)^{-1} \quad 3.3$$

And the equivalent radius of the system as

$$R_e = \left(\frac{4}{d_1} + \frac{4}{d_2}\right)^{-1} \quad 3.4$$

Then equation 3.1 can be expressed as:

$$r = \sqrt[3]{\frac{3FR_e}{2E_e}} \quad 3.5$$

The deflection of the system due to elastic deformation of the bodies at the contact interface, δ, as defined in Figure 18 is

$$\delta = \frac{1}{2}\left(\frac{1}{R_e}\right)^{1/3}\left(\frac{3F}{3E_e}\right)^{2/3} \quad 3.6$$

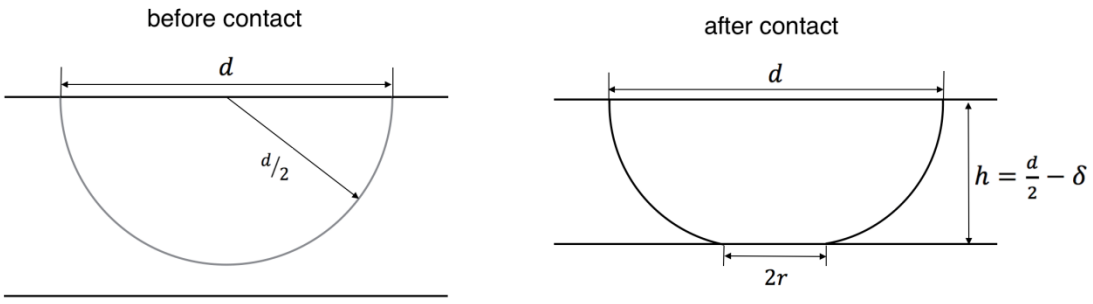

Figure 18 Relationship between distance from hydrogel base to surface (h), contact radius (r), and hemisphere diameter (d).

Combining equations 3.5 and 3.6, we get

$$r = 2\delta R_e{}^{2/3} \qquad 3.7$$

Which predicts a linear relationship between vertical deformation of the hemisphere and the contact radius formed. Interestingly, this relationship is independent of material properties and is only a function of geometric parameters.

The maximum pressure, $\mathcal{P}_{max}$, occurs at the center of the contact area:

$$\mathcal{P}_{max} = \frac{3F}{2\pi r^2} \qquad 3.8$$

The maximum stresses occur on the *z* axis, and these are principal stresses. Their values are:

$$\sigma_1 = \sigma_2 = \sigma_x = \sigma_y$$

$$= -\mathcal{P}_{max}\left[\left(1 - \left|\frac{z}{r}\right|\tan^{-1}\frac{1}{\left|\frac{z}{r}\right|}\right)(1+\nu) - \frac{1}{2(1+\frac{z^2}{r^2})}\right] \qquad 3.9$$

$$\sigma_3 = \sigma_z = \frac{-\mathcal{P}_{max}}{1 + \frac{z^2}{r^2}} \qquad 3.10$$

since $\sigma_1 = \sigma_2$, we have $\tau_{12} = 0$ and

$$\tau_{max} = \tau_{13} = \tau_{23} = \frac{\sigma_1 - \sigma_3}{2} = \frac{\sigma_2 - \sigma_3}{2} \qquad 3.11$$

Figure 19 is a plot of equations 3.9, 3.10, and 3.11 for a distance to $3r$ below the surface. If we consider the Poisson's ration of PEG to be 0.18 [38], the shear stress reaches its maximum value at a distance $z = 0.45r$ below the surface, where it is approximately equal to $0.34\mathcal{P}_{max}$.

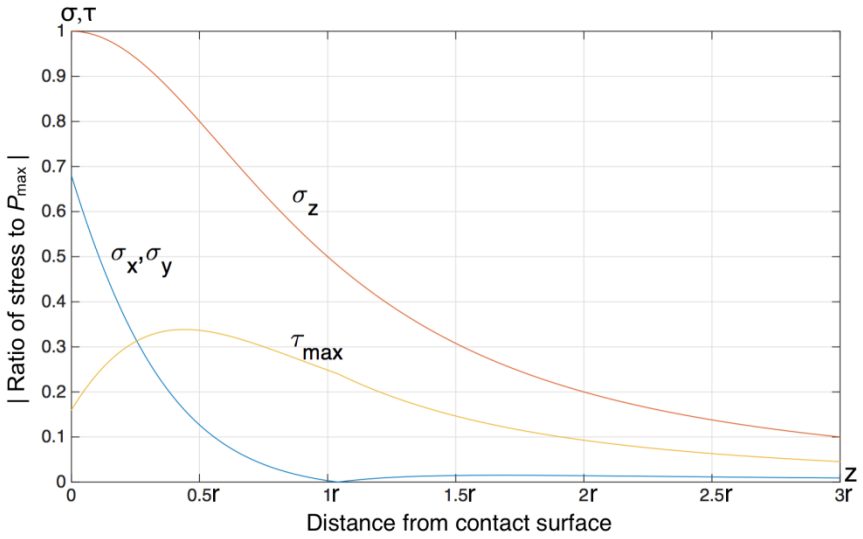

Figure 19 Magnitude of the stress components below the surface as a function of the maximum pressure of contacting sphere.

Thus we have

$$\tau_{max} = 0.34\mathcal{P}_{max} = 0.34 \times \frac{3F}{2\pi r^2} \qquad 3.12$$

If we consider material failure to occur when the shear stress exceeds the shear strength of the material, i.e., when $\tau_{max} \leq 0.5S_y$, it is possible to use this relation and equation 3.5 and 3.12 to find the radius of the largest possible contact circle that could be produced before the material failed; the radius of this circle would be:

$$r_{max} = \frac{\pi}{0.68} S_y \frac{R_e}{E_e} \qquad 3.13$$

It should be noted that the properties of the PEG used in this work, like Elastic Modulus (E) and yield strength (S_y), are difficult find in literature or predict *a priori* because they are highly dependent on individual fabrication parameters (molecular weight of PEG chains, % crosslinking, % water, etc.). However, in the future we can measure these properties experimentally for a given PEG formulation and use the equations derived here to predict deformation of PEG once the properties are known.

3.2 Solute Diffusion within Hydrogels

Hydrogels are hydrophilic polymers comprised of a nanoscale network of polymer chains. Thermosetting hydrogels have chemical cross-links between the chains, and when these materials are saturated with water, the chains and cross-links form a nanoscale mesh through which water and solutes can diffuse. The density of this mesh plays an important role in governing solute movement within hydrogels.

The rate of solute diffusion through a hydrogel increases as the density of cross-links within the hydrogel decreases, the length of polymer chains increases, or the volumetric concentration of water in the hydrogel increases. All of these factors cause a decrease in the mesh density of the hydrogel to some degree. The speed of solute diffusion through a hydrogel network can be described using a "hindered" diffusion coefficient in the hydrogel (D_g) relative to that of the "free" diffusion of the solute in solution (D_o).

There are a number of models that have been used to describe the ratio between hindered and free diffusion [40]; one of the most common models depends on the solute radius (r_s) relative to the characteristic length a of a cross-linked hydrogel network (ξ). In addition, the equilibrium water content of the hydrogel network has an effect, described here as the polymer volume fraction in the gel (V_f), which is the inverse of the equilibrium swelling ratio of hydrogel [41].

$$\frac{D_g}{D_o} = \left(1 - \frac{r_s}{\xi}\right) \exp\left[-Y\left(\frac{V_f}{1 - V_f}\right)\right] \qquad 3.14$$

where Y is the ratio of the critical volume required for a successful translational movement of the solute to the average free volume per liquid molecule and is usually approximated to be 1.

The hindered diffusion coefficient is often difficult to calculate *a priori* because the characteristic length can be challenging to predict in a hydrogel. Thus, this coefficient

is often determined experimentally by using an apparatus such as the blind-well chambers shown in figure 20.

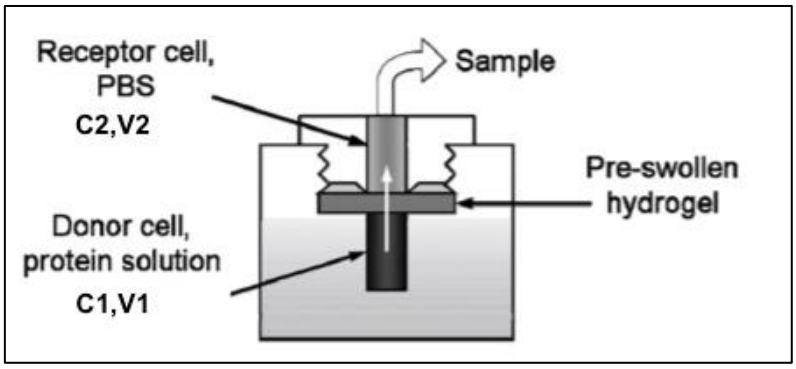

Figure 20 Model of blind-well chambers; from [42].

The blind-well system is comprised of two chambers separated by a thin hydrogel membrane. Solute diffuses from the high-concentration "donor cell" with a solute concentration of C_1 through the hydrogel and into the "receptor cell", which has an solute concentration of C_2. By measuring the concentration in the receptor cell as a function of time, it is possible to calculate the hindered diffusion coefficient of the solute in the hydrogel. In using the blind-well system the following assumptions are made:

i. The chamber solutions are well mixed so that there is no concentration gradient within either solution.
ii. Solute diffusion is one-dimensional through the hydrogel, so lateral diffusion within the gel can be neglected
iii. There is no accumulation of solute at the surfaces of the hydrogel

iv. The diffusion coefficient of protein D_g is independent of the solute concentration

When the experiment begins, the solute concentration in the receptor cell is zero ($C_2 = 0$ at $t = 0$), but increases slowly over time. By sampling the receptor cell concentration at various timepoints and the above assumptions, it is possible to calculate the hindered diffusion coefficient using the following relation [43]:

$$\frac{C_2}{N/V} = \frac{D_g t}{h\tau} \qquad 3.15$$

where h is the thickness of the hydrogel membrane, and t is time. N is total number of moles of solute in the system and V and τ describe geometric parameters of the system; these parameters can be calculated as follows [43]:

$$N = C_1\left(V_1 + \frac{Ah}{2}\right) + C_2\left(V_2 + \frac{Ah}{2}\right) \qquad 3.16$$

and

$$V = V_1 + Ah + V_2 \qquad 3.17$$

$$\tau = \frac{(V_1 + Ah/2)(V_2 + Ah/2)}{AV} \qquad 3.18$$

where V_1 and V_2 are the volumes of the donor and receptor cell, respectively, and A is the contact area between the hydrogel membrane and chamber of the receptor cell. In future work, this method will be used to determine the diffusion coefficient of different formulations of PEG, which will be used to build a predictive model of protein motion in the hydrogel.

Chapter 4 Experimental Device Design

4.1 Microcontact Printing System

The microcontact printing system was designed to hold a hydrogel stamp and glass target surface so that the distance between the two could be precisely controlled, and so that the entire printing process could be observed in real-time on an inverted fluorescent microscope. When using the system, shown in Fig. 21, the glass target surface rests on the base platform/microscope stage component, while the z-stage is used to lower the hydrogel (fixed inside the hydrogel printing platform) into contact. A viewing window in the bottom of the base platform/microscope stage allows the entire process to be observed optically from below.

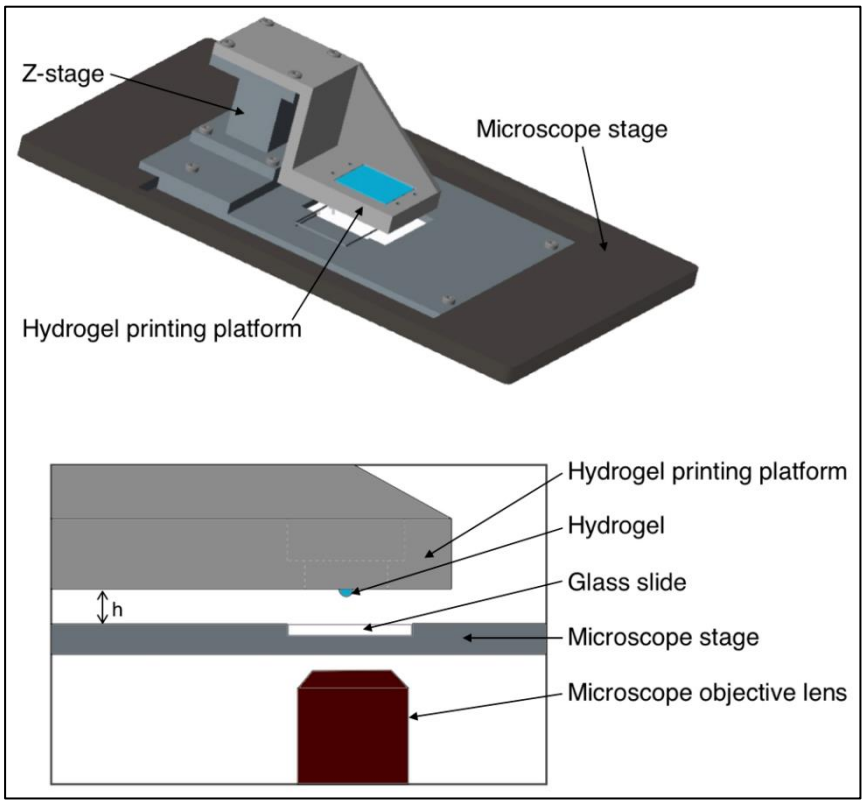

Figure 21 Drawing of assembled microcontact printing system.

The microcontact printing system includes three main parts: (1) a base component that attaches the system to an inverted microscope and holds the glass target surface, (2) a platform designed to hold the hydrogel stamp and (3) a precision vertical translation stage (z-stage) that connects the two. The base component (Fig. 22) was fabricated to fit onto a Nikon Ti-E inverted microscope; the base was machined out of aluminum by the Mechanical Engineering machine shop. The z-stage was also purchased commercially (T40Z-10A, MPositioning CO., LTD., Fig. 23); it was made of aluminum alloy and has a travel distance of 10 mm, resolution of 10 µm, and accuracy of 10 µm.

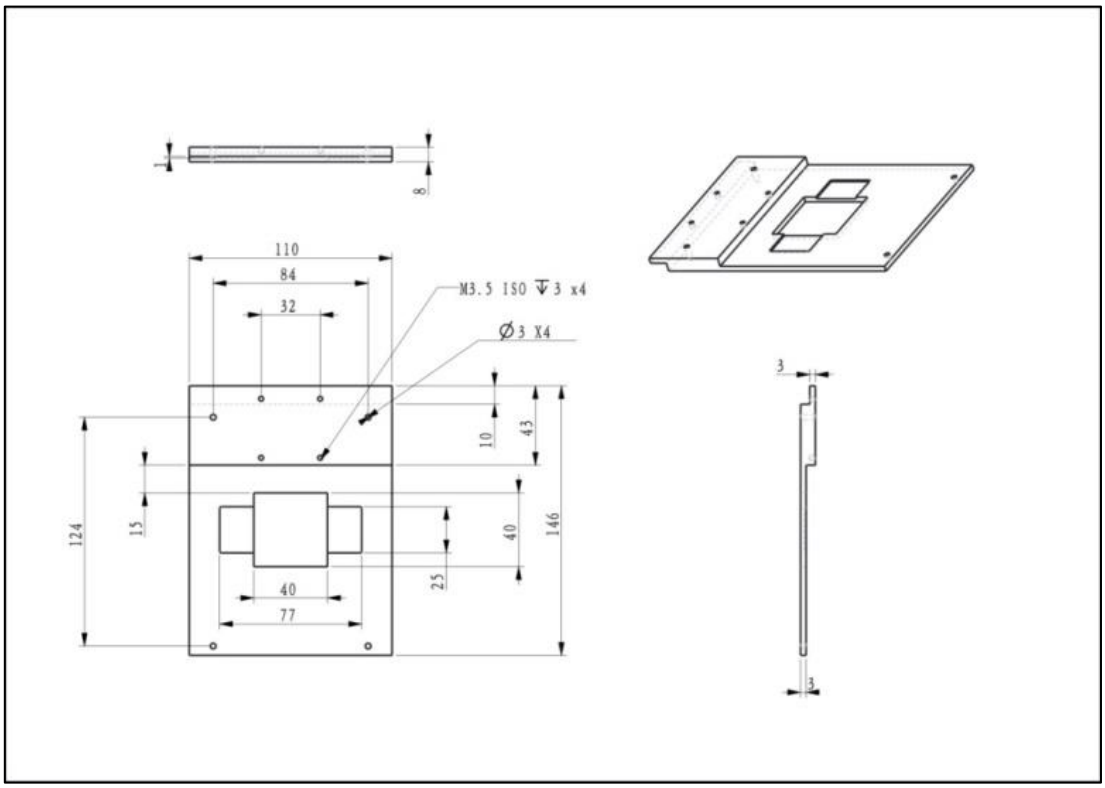

Figure 22 Base printing platform that attached to the microscope stage, all dimensions in millimeters

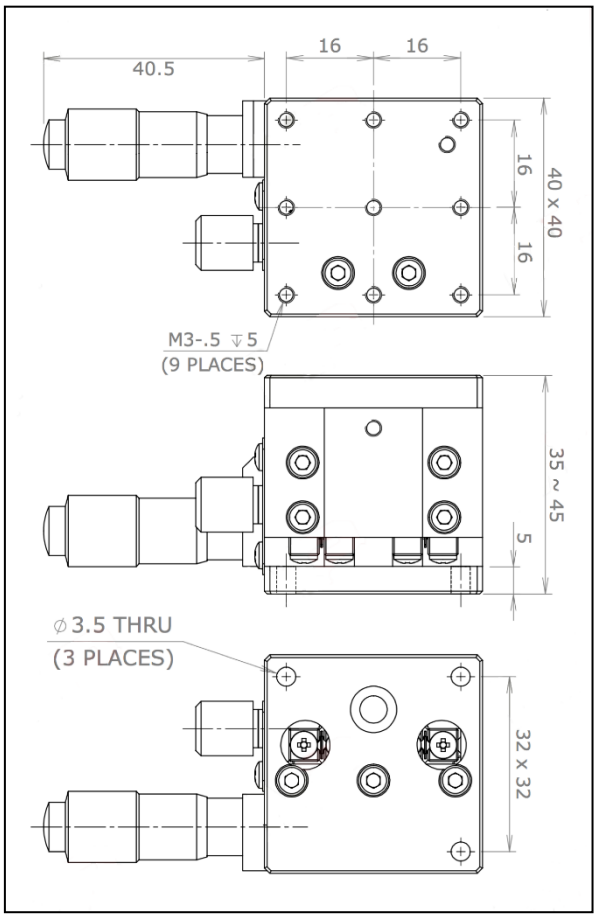

Figure 23 Precision z-stage (Dimensioned drawing provided by manufacturer), all dimensions in millimeters.

The hydrogel stamp platform (Figure 24) was designed to provide a stable base for holding the hydrogel stamps during printing. The s-shaped design allows it to bolt to the top of the z-stage, so that actuating the stage will control the distance between the hydrogel stamp and the target glass surface. This component was machined at the Mechanical Engineering departmental machine shop out of aluminum.

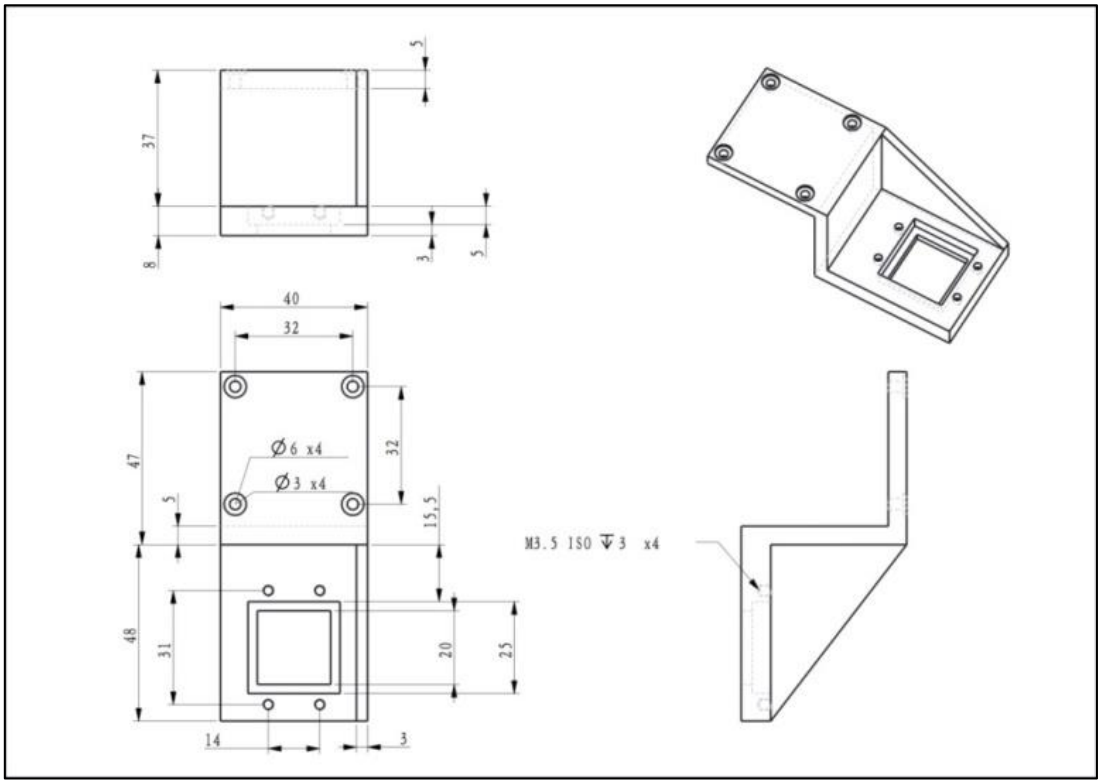

Figure 24 Hydrogel stamp platform; all dimensions in millimeters.

Chapter 5 Protein Printing

5.1 Creation of Hemispherical PEG Hydrogel Stamp using PDMS Mold

The hemispherical hydrogel stamps were made using a three-step process. First, a metal sphere and laser-cut acrylic components were assembled to make a mold cavity (Fig. 25 A and B). Then, polydimethylsiloxane (PDMS) prepolymer was poured into this cavity and cured in order to form a negative mold (Fig. 25 C). Finally, this PDMS mold was combined with acrylic pieces to build a cavity for molding the PEG hydrogel; a liquid PEG solution is poured into this cavity and crosslinked, resulting in a final PEG stamp with a hemispherical protrusion (Fig. 25 D).

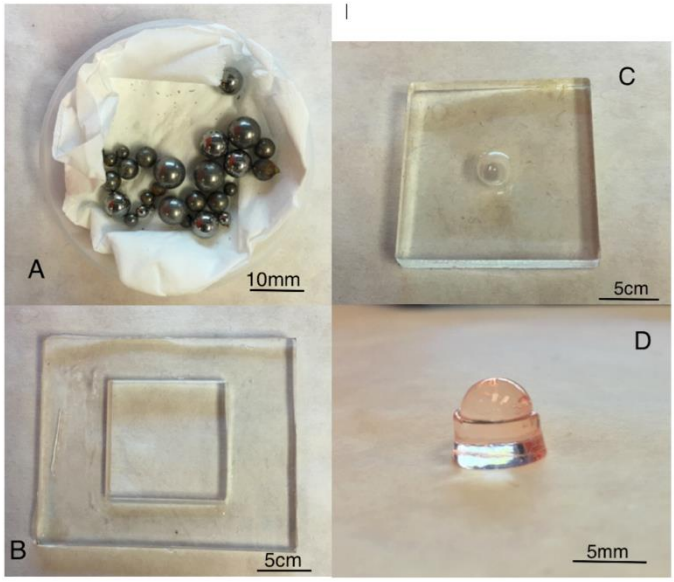

Figure 25 (A) Metal spheres with different diameters used for making the initial mold cavity. (B) One of the laser-cut acrylic pieces. (C) PDMS mold. (D) Hemispherical PEG.

5.1.1 Creation of PDMS Mold

The first step in creating the hydrogel stamps was to make the cavity for generating a

PDMS mold. To do this, a 2 mm thick acrylic sheet was cut into a 45 mm × 55 mm piece with a 4.8 mm diameter hole in the center using a laser cutter. A 5 mm diameter metal ball was installed into the 4.8 mm hole, creating a force-fit between the components so that the metal ball only partially protruded through the hole. A 4 mm thick acrylic sheet was cut into a 45 mm × 55 mm piece with a 20 mm × 20 mm square window in the center using laser cut machine. All of these components and one 75mm × 50mm glass microscope slide were rinsed with IPA (Isopropanol(CH_3)CHOH), followed by a second rinse with water, and then dried under a stream of air. These components would eventually form the mold cavity into which liquid PDMS prepolymer would be poured and cured in order to form the PDMS mold.

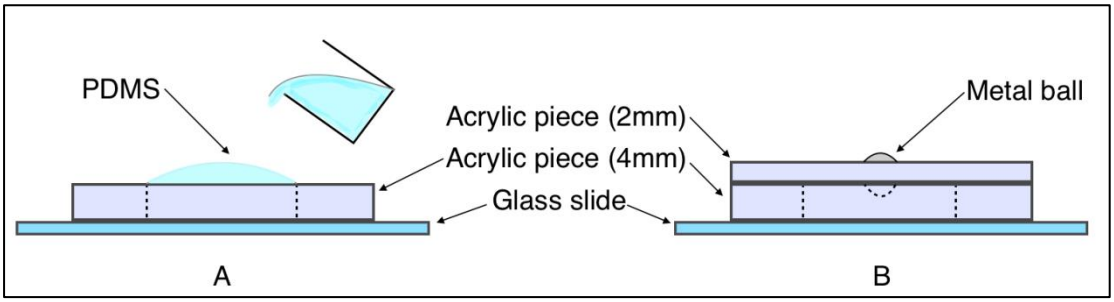

Figure 26 Preparation of PDMS hemispherical mold.

To make the PDMS mold, PDMS (Sylgard 184, Dow Corning) was prepared by combining the silicon base and the curing agent with 10:1 ratio in a clean plastic cup and stirred vigorously for 3 minutes. The mixture was then degassed by placing it in a vacuum (Thermo Scientific) for 2 hours, making sure there were no air bubbles

before removing it from the vacuum. The degassed PDMS liquid was carefully and slowly poured into the cavity created by the glass slide and 4 mm thick acrylic piece, as shown in Figure 26 A, making sure that the PDMS completely filled the cavity. The 2mm thick acrylic piece and metal ball were then used to completely enclose the cavity, being sure that there were no air bubbles entrapped during the process, as shown in Figure 26 B. Two binder clips were applied to clamp the assembly together. The whole assembly was then placed in an oven (Quincy 40 GC lab oven) at 65 degrees Celsius for 2 hours to cross-link the PDMS. Once set, the assembly was removed from the oven and allowed to cool to room temperature, followed by slowly and gently removing the final PDMS mold.

5.1.2 Fabrication of Hemispherical PEG Hydrogel Stamp

Once the PDMS mold was prepared, it was used to create the PEG hydrogel stamp. First, a liquid prepolymer of 20% (wt/wt%) PEG was prepared using the following method: 0.25 g Polyethylene glycol diacrylate (PEG, Molecular Weight = 8000 DA, Alfa Aesar) was measured on a balance with a weighting paper and added to a 1.5 ml microcentrifuge tube. 1 ml deionized water (DI-water purified from Milli-Q® Direct Water Purification System, EMD Millipore Corporation) and 0.013 g 2-Hydroxy-2-methylpropiophenone photoinitiator (Sigma-Aldrich) were also added to the microcentrifuge tube. The solution was then mixed using a vortex generator (Vortex Genie 2, Scientific Industries) at 3000 rpm for 4 minutes.

The liquid prepolymer solution was then used to create a hemispherical PEG stamp

by pouring it into the PDMS mold. In order to accomplish this, a 2 mm thick acrylic sheet was cut into a 45 mm × 55 mm piece with a 5.5 mm diameter hole in the center. This 2 mm thick acrylic piece, two 75mm × 50mm glass slides, the PDMS mold, and the 4 mm thick acrylic piece used in making the PDMS mold were rinsed thoroughly with IPA, then rinsed with water and dried under a steam of air. One of the glass slides, the PDMS mold, and both acrylic pieces were assembled as shown in Figure 27 A. Then the prepolymer solution was introduced into the well formed by the PDMS mold and the hole in the 2 mm thick acrylic piece. The second glass slide was used cover the top surface, as shown in Figure 27 B, taking care to avoid the introduction of any air bubble during the processes. Two binder clips were used to clamp together the entire assembly, which was then exposed under long wave UV light (2.33 MW/cm^{2}model UVGL-25, UVP Incorporation) for 4 minutes to initiate cross-linking of the PEG.

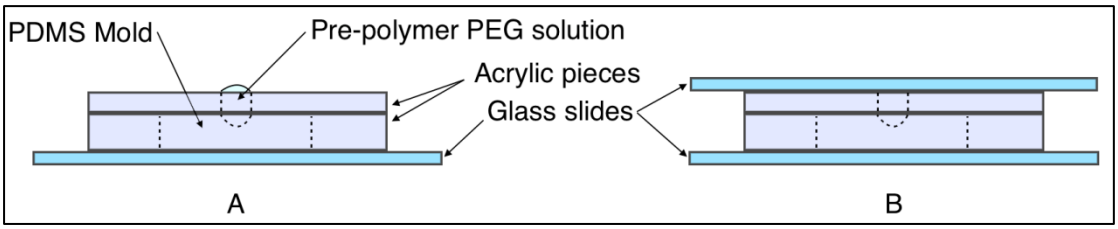

Figure 27 Preparation of Hemispherical PEG Hydrogel Stamp.

After crosslinking, the PEG stamp was gently and slowly removed from the assembly, avoiding any breakage because the PEG is low strength. After removal from the molds, PEG stamps were soaked into DI water for 1 hour to reach equilibrium.

Prior to being used in stamping experiments, PEG stamps were removed from the DI water and soaked in a solution of 0.1 mg/mL Avidin labeled with fluorescent Tetramethylrhodamine (Avidin-TRITC 2 mg/ml, Protein Mods) for 8 hours until the internal protein concentration equilibrated.

5.2 Preparation of Target Surface

All patterning experiments were performed on glass surfaces that were pretreated to facilitate protein binding. Glass surfaces were functionalized with Biotin-PEG-Silane, as shown in Fig. 28: when these molecules are introduced to a glass surface, the silane group preferentially binds to the glass surface. These molecules align to form a close-packed monolayer that is covered with Biotin groups. Biotin and Avidin proteins experience strong preferential binding [44] so this surface is ideal for capturing Avidin during the microcontact printing process.

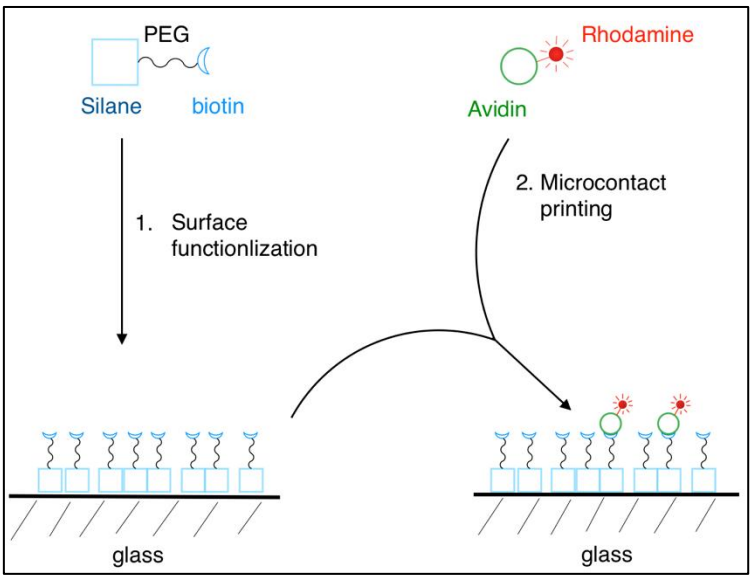

Figure 28 Schematic of glass surface functionalization and fluorescent tagged protein attachment.

The specific process for functionalizing the glass surfaces is as follows. Glass microscope cover slips (22 mm × 40 mm x 0.17 mm Thermo Scientific) were cleaned using IPA followed by water and then dried under a steam of air. 0.95 ml of Ethanol (100%, Sigma-Aldrich) and 0.5 ml DI water were added to 1.5 ml microcentrifuge tube. 3-4 µg of Biotin-PEG-Silane (Molecular Weight = 5000, Laysan Bio, Inc.) was measured on the balance using weighing paper and added to the water/ethanol mixture. The solution was mixed by vortexing for 2 minutes. The well-mixed solution was then pipetted onto the surface of the microscope cover glass and retained there for 30 minutes, allowing the Biotin-PEG-Silane molecules time to bind to the glass surface. During this time, the microscope cover glass was coved with a plastic container to prevent evaporation of the solution. Afterwards, the microscope cover glass was rinsed thoroughly with Phosphate Buffer Saline solution (PBS without calcium and magnesium, Mediatech, Inc) and dried under a stream of air. The surfaced-treated microscope cover slips were always labeled with the date of fabrication on the corner, which also made it possible to distinguish between the treated and untreated surface. Surface-treated microscope cover slips were prepared freshly before every experiment.

5.3 Uniform-Concentration Protein Printing

The purposes of this set of experiments was to demonstrate that proteins could be deposited on surfaced-treated microscope cover glass and that different density of proteins could be printed by controlling the amount of contact time between the hydrogel stamp and functionalized glass.

To perform these experiments, first a cleaned glass slide was installed on the base printing platform in order to provide an optically-transparent rigid surface, and a freshly-prepared pre-treated microscope cover glass was placed on top of it. A hemispherical PEG hydrogel stamp was then removed from protein solution, rinsed with DI water to remove residual protein on the surface, and then the surface was dried briefly using a stream of air. The hydrogel was installed onto the hydrogel printing platform and then stamped onto a sacrificial section of the pre-treated glass for 1 second to remove any remaining residual proteins on the surface. Then the stamps were brought into contact with a clean region of the pre-treated glass surface for the specified amount of time. After printing, pre-treated glass surface was rinsed by DI water and dried under a stream of air, then all surfaces were imaged on a Nikon fluorescence microscope (Nikon ECLIPSE Ti) using TRITC fluorescent filters, and analyzed using NIS-Elements AR software to determine fluorescent intensity.

Because PEG can shrink as it dehydrates after long exposure to ambient air conditions, the experimental setup (including the hydrogel printing platform, z-stage and microscope stage) was enclosed in a stainless steel cylinder with a portable humidifier to control the humidity and prevent the hydrogel from dehydrating.

A sample image, shown in Fig. 29 was obtained from a 5-minute printing time. The image shows relatively uniform intensity in the contact region, indicating that Avidin

diffused from the PEG hydrogel to the surface of the pre-treated glass and bound with Biotin on the surface of pre-treated glass at a relatively uniform rate over the contact area. Some bright spots were occasionally observed during printing, such as the one seen in the upper-left hand corner of Figure 29; these spots were attributed to defects in the hydrogel material and/or local crystallization of the Avidin protein.

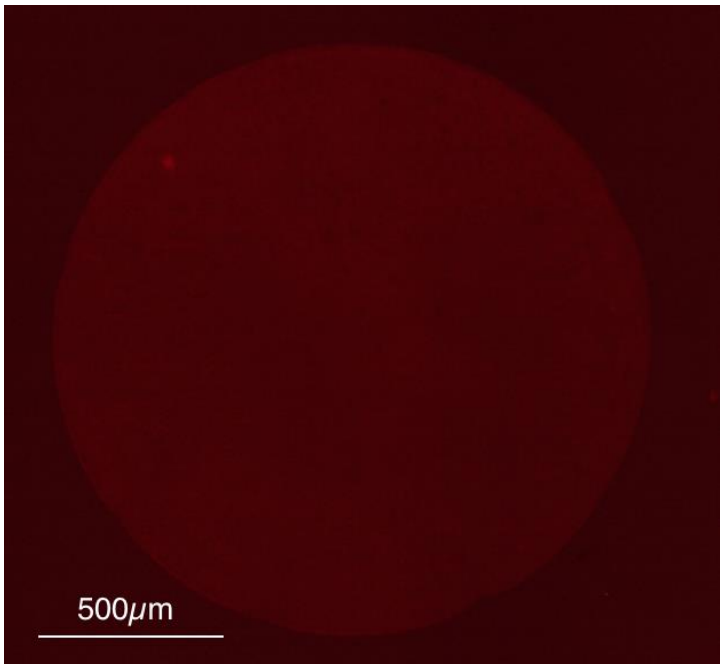

Figure 29 Fluorescent image resulting from single-step printing of hydrogel for 5 minutes.

This experiment was repeated with contact times of 5 seconds, 10 seconds, 20 seconds and 30 seconds. Comparing light intensity of these four contact times, there was no statistical difference. Then, the contact experiment was repeated for 1 minute, 2 minutes, 5 minutes, 10 minutes, 15 minutes and 20 minutes. Five independent experiments were performed and measured for each contact time.

The results of this experiment are shown in Figure 30; each data point represents the mean value obtained in the five independent experiments. As contact time increases from 30 seconds to 20 minutes, the fluorescent intensity increases, showing that the density of protein deposited on pre-treated glass slides increased. Contact times between 1 and 10 minutes showed the greatest difference in protein deposition, but after 15-20 minutes, the surfaces appear to reach saturation as free biotin keys on the pre-treated glass were fully bound with fluorescently-tagged Avidin. Surfaces printed for longer than 20 minutes displayed the same fluorescent intensity as those printed for 20 minutes.

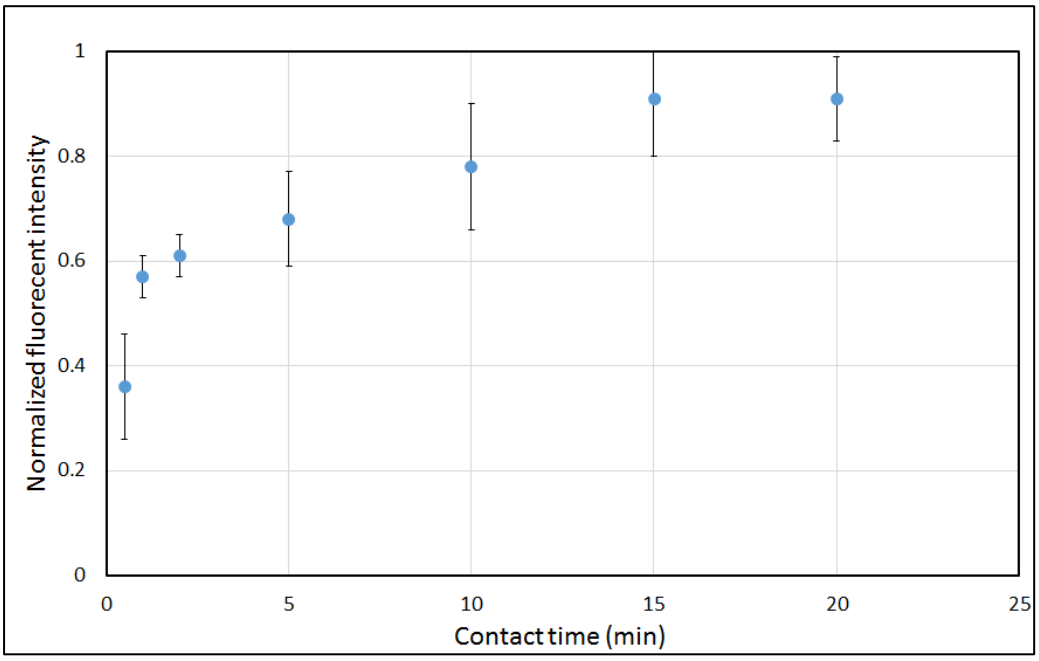

Figure 30 Normalized fluorescent intensity versus contact time.

Table 1 Fluorescent intensity profile.

Contact Time (min)	Normalized fluorescent intensity
0.5	0.36
1	0.57
2	0.61
5	0.68
10	0.78
15	0.91
20	0.91

5.4 Multi-step Protein Printing

Using the knowledge gained from the previous set of experiments combined with the low elastic modulus of the PEG hydrogel, it was possible to generate multiple-density surface patterns, such as the one shown in Fig. 31. For this experiment, the hydrogel was initially brought into contact with the pre-treated glass under low pressure for 9 minutes, then the pressure was increased and held there for an additional minute. This resulted in a contact time in the center of the pattern of 10 minutes, while the outer ring was only in contact for 1 minute. The resulting fluorescent image (Fig. 31) shows a significant difference in fluorescence intensity observed between the center region (high contact time) and outer region (low contact time) of the print.

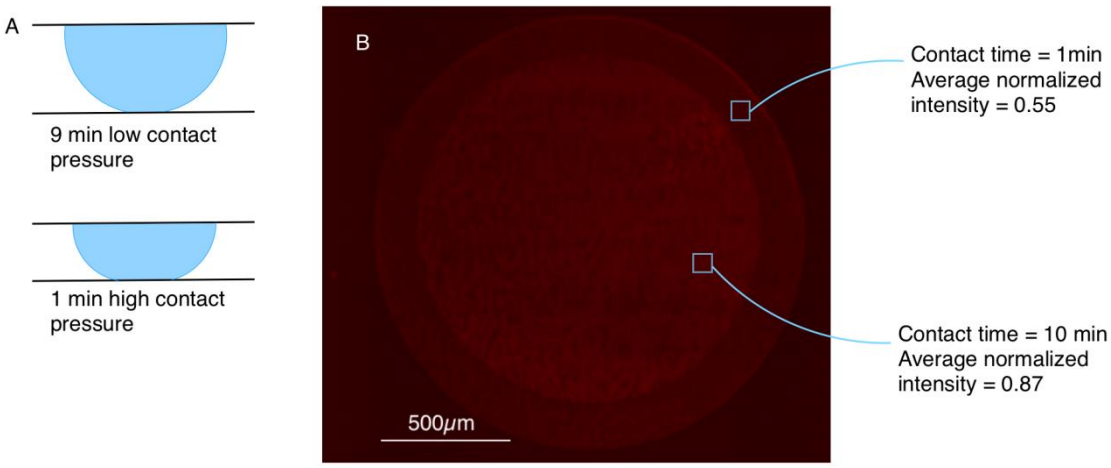

Figure 31 Dual pressure protein printing.

Using the same methodology and the data from Table 1, a four-step protein print was created as shown in Fig. 32. By reducing contact pressure step by step, the stamp was held at the highest pressure for 30 seconds, followed by a decreased pressure for 1 minute 30 seconds, a second decrease in pressure for 6 minutes, and finally the lowest pressure for 14 minutes. This resulted in a contact time for each layer of 30 seconds, 2 minutes, 8 minutes, and 20 minutes.

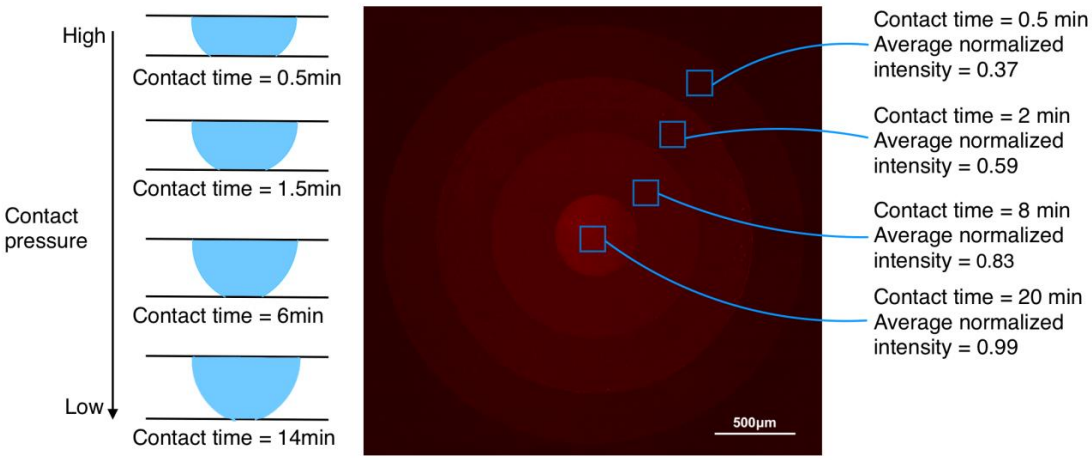

Figure 32 Multiple pressure protein printing. Contact time from outer to inner are 30s, 2 min, 8min, and 20 min.

The intensity values in the 4-step printing process showed good agreement with the individual intensity values obtained with the homogeneous printing process in section 5.3. Based on these results, with automated control of contact time it may be possible to create controllable surface gradients. Eventually integrating this method with more complex mold topography could pave the way for true gray-scale microcontact printing of proteins.

Chapter 6 Conclusions and Future Work

6.1 Conclusions

The work described in this thesis focused on the design and fabrication of 3D PEG hydrogel stamps and the use of this PEG to generate single-concentration or multiple-concentration protein surface patterns. As presented conceptually in Chapter 3, by controlling the contact time between a hydrogel stamp and target surface, it is possible to control the rate of protein deposition onto the surface. Combining this concept with controlled deformation of a 3D low-modulus hydrogel stamp, it becomes possible to print homogeneous and heterogeneous protein patterns on a surface. In order to make this possible, a platform was created to control contact pressure of the stamp, as outlined in Chapter 4. Then this device was used to create homogeneous and heterogeneous patterns of proteins, as outlined in Chapter 5. This method demonstrates an approach that can be used to generate protein arrays with controlled density, and used to generate complex micro-contact printed protein surfaces.

6.2 Future Work

The research presented in this thesis presents a novel method for using 3D hydrogel stamps to generate multiple-density protein surface patterns. The negative PDMS mold used in this demonstration was a simple hemisphere, but using other fabrication methods, such as 3D printing, it is possible to generate much more complex mold topography, which in turn can be used to generate more complex surface patterns. In addition, while a single feature was demonstrated in this work, the stamping process provides the possibility of parallel printing of multiple identical or unique patterns simultaneously. Finally, using the knowledge gained regarding the protein diffusion within the PEG hydrogel and the relationship between contact time with protein intensity, with automated control of contact pressure over time, it opens up the possibility to use this method to print surface patterns with concentration gradients rather than the multi-stepped patterns demonstrated here.

References

[1] A. Kumar and G. Whitesides, "Features of gold having micrometer to centimeter dimensions can be formed through a combination of stamping with an elastomeric stamp and an alkanethiol ink followed by chemical etching," *Applied Physics Letters,* vol. 63, no. 14, pp. 2002-2004, 1993.

[2] A. Bernard, E. Delamarche, H. Schmid, B. Michel, H. R. Bosshard and H. Biebuyck, "Pringting Patterns of Protein," *Langmuir,* vol. 14, pp. 2225-2229, 1998.

[3] C. D. James, R. C. Davis, L. Kam, H. G. Craighead, M. Isaacson, J. N. Turner and W. Shain, "Pattern protein layers on solid substrate by thin stamp microcontact printing," *Langmuir,* vol. 14, pp. 741-744, 1998.

[4] N. Patel, R. Bhandari, K. M. Shakesheff, S. M. Cannizzaro, M. C. Davies, R. Langer, C. J. Roberts, S. J. Tendler and P. M. J. Williams, "Printing patterns of biospecifically-adsorbed protein," *Biomater. Sci., Polym. Ed,* vol. 11, pp. 319-331, 2000.

[5] B. D. Martin, B. P. Gaber, C. H. Patterson and D. C. Turner, "Direct Protein Microarray Fabrication Using a Hydrogel 'Stamper'," *Langmuir,* vol. 14, no. 15, pp. 3971-3975, 1998.

[6] Delamarche, E., Bernard, A., Schmid, H., Bietsch, A., Michel, B. and Biebuyck, H, "Microfluidic networks for chemical patterning of substrates: design and application to bioassays," *Journal of the American Chemical Society,* vol. 120, no. 3, pp. 500-508, 1998.

[7] Delamarche, E., Bernard, A., Schmid, H., Michel, B. and Biebuyck, H, "Patterned delivery of immunoglobulins to surfaces using microfluidic networks," *Science,* vol. 276, no. 5313, pp. 779-781, 1997.

[8] Patel, N., Sanders, G.H., Shakesheff, K.M., Cannizzaro, S.M., Davies, M.C., Langer, R., Roberts, C.J., Tendler, S.J. and Williams, P.M, "Atomic force microscopic analysis of highly defined protein patterns formed by microfluidic networks," *Langmuir,* vol. 15, no. 21, pp. 7252-7257, 1999.

[9] Caelen, I., Bernard, A., Juncker, D., Michel, B., Heinzelmann, H. and Delamarche, E, "Formation of gradients of proteins on surfaces with microfluidic networks," *Langmuir,* vol. 16, no. 24, pp. 9125-9130, 2000.

[10] A. Bernard, J. P. Renault, B. Michel, H. R. Bosshard and E. Delamarche, "Microcontact printing of proteins," *Adv. Mater.,* vol. 12, pp. 1067-1070, 2000.

[11] Papra, A., Bernard, A., Juncker, D., Larsen, N.B., Michel, B. and Delamarche, E, "Microfluidic networks made of poly (dimethylsiloxane), Si, and Au coated with polyethylene glycol for patterning proteins onto surfaces," *Langmuir,* vol. 17, no. 13, pp. 4090-4095, 2001.

[12] Chiu, D.T., Jeon, N.L., Huang, S., Kane, R.S., Wargo, C.J., Choi, I.S., Ingber, D.E. and Whitesides, G.M, "Patterned deposition of cells and proteins onto surfaces by using three-dimensional microfluidic systems," *Proceedings of the National Academy of Sciences,* vol. 97, no. 6, pp. 2408-2413, 2000.

[13] Jeon, N.L., Choi, I.S., Xu, B. and Whitesides, G.M, "Large-area patterning by vacuum-assisted micromolding," *Advanced Materials,* vol. 11, no. 11, pp. 946-950, 1999.

[14] Folch, A., Ayon, A., Hurtado, O., Schmidt, M.A. and Toner, M, "Molding of deep polydimethylsiloxane microstructures for microfluidics and biological applications," *Journal of Biomechamical Engineering,* vol. 121, no. 1, pp. 28-34, 1999.

[15] A. Folch and M. Toner, "Cellular micropatterns on biocompatible materials," *Biotechnology progress,* vol. 14, no. 3, pp. 388-392, 1998.

[16] Barron, J.A., Young, H.D., Dlott, D.D., Darfler, M.M., Krizman, D.B. and Ringeisen, B.R, "Printing of protein microarrays via a capillary-free fluid jetting mechanism," *Proteomics,* vol. 5, no. 16, pp. 4138-4144, 2005.

[17] Nishizuka, S., Charboneau, L., Young, L., Major, S., Reinhold, W.C., Waltham, M., Kouros-Mehr, H., Bussey, K.J., Lee, J.K., Espina, V. and Munson, P.J, "Proteomic profiling of the NCI-60 cancer cell lines using new high-density reverse-phase lysate microarrays," *Proceedings of the National Academy of Sciences,* vol. 100, no. 24, pp. 14229-14234, 2003.

[18] Michaud, G.A., Salcius, M., Zhou, F., Bangham, R., Bonin, J., Guo, H., Snyder, M., Predki, P.F. and Schweitzer, B.I, "Analyzing antibody specificity with whole proteome microarrays," *Nature biotechnology,* vol. 21, no. 12, pp. 1509-1512, 2003.

[19] MacBeath, G. and Schreiber, S.L, "Printing proteins as microarrays for high-throughput function determination," *Science,* vol. 289, no. 5485, pp. 1760-1763, 2000.

[20] J. A. Barron, B. J. Spargo and B. R. Ringeisen, "Biological laser printing of three dimensional cellular structures," *Applied Physics A,* vol. 79, no. 4-6, pp. 1027-1030, 2004.

[21] Hypolite, C.L., McLernon, T.L., Adams, D.N., Chapman, K.E., Herbert, C.B., Huang, C.C., Distefano, M.D. and Hu, W.S., "Formation of microscale gradients of protein using heterobifunctional photolinkers," *Bioconjugate chemistry,* vol. 8, no. 5, pp. 658-663, 1997.

[22] A. Folch and M. Toner, "Cellular micropatterns on biocompatible materials," *Biotechnology progress,* vol. 14, no. 3, pp. 388-392, 1998.

[23] Caelen, I., Gao, H. and Sigrist, H, "Protein density gradients on surfaces," *Langmuir,* vol. 18, no. 7, pp. 2463-2467, 2002.

[24] Fosser, K.A. and Nuzzo, R.G, "Fabrication of patterned multicomponent protein gradients and gradient arrays using microfluidic depletion,"

Analytical chemistry, vol. 75, no. 21, pp. 5775-5782, 2003.

[25] Monahan, J., Gewirth, A.A. and Nuzzo, R.G, "A method for filling complex polymeric microfluidic devices and arrays," *Analytical chemistry,* vol. 73, no. 13, pp. 3193-3197, 2001.

[26] S. K. W. Dertinger, X. Jiang, Z. Li, V. N. Murthy and a. G. M. Whitesides, "Gradients of substrate-bound laminin orient axonal specification of neurons," *Proceedings of the National Academy of Sciences,* vol. 99, no. 20, pp. 12542-12547, 2002.

[27] Mayer, M., Yang, J., Gitlin, I., Gracias, D.H. and Whitesides, G.M, "Micropatterned agarose gels for stamping arrays of proteins and gradients of proteins," *Proteomics,* vol. 4, no. 8, pp. 2366-2376, 2004.

[28] Shi, J., Wang, L., Zhang, F., Li, H., Lei, L., Liu, L. and Chen, Y, "Incorporating protein gradient into electrospun nanofibers as scaffolds for tissue engineering," *ACS applied materials & interfaces,* vol. 2, no. 4, pp. 1025-1030, 2010.

[29] Krämer, S., Xie, H., Gaff, J., Williamson, J.R., Tkachenko, A.G., Nouri, N., Feldheim, D.A. and Feldheim, D.L., "Preparation of protein gradients through the controlled deposition of protein-nanoparticle conjugates onto functionalized surfaces," *Journal of the American Chemical Society,* vol. 126, no. 17, pp. 5388-5395, 2004.

[30] Liedberg, B. and Tengvall, P., "Molecular gradients of. omega.-substituted alkanethiols on gold: preparation and characterization," *Langmuir,* vol. 11, no. 10, pp. 3821-3827, 1995.

[31] Liedberg, B., Wirde, M., Tao, Y.T., Tengvall, P. and Gelius, U., "Molecular gradients of ω-substituted alkanethiols on gold studied by X-ray photoelectron spectroscopy," *Langmuir,* vol. 13, no. 20, pp. 5329-5334, 1997.

[32] Ruardy, T.G., Schakenraad, J.M., Van der Mei, H.C. and Busscher, H.J., "Adhesion and spreading of human skin fibroblasts on physicochemically characterized gradient surfaces," *Journal of biomedical materials research,* vol. 29, no. 11, pp. 1415-1423, 1995.

[33] Ruardy, T.G., Moorlag, H.E., Schakenraad, J.M., Van Der Mei, H.C. and Busscher, H.J., "Growth of fibroblasts and endothelial cells on wettability gradient surfaces," *Journal of colloid and interface science,* vol. 188, no. 1, pp. 209-217, 1997.

[34] S. Daniel, M. K. Chaudhury and a. J. C. Chen, "Fast drop movements resulting from the phase change on a gradient surface," *Science,* vol. 291, no. 5504, pp. 633-636, 2001.

[35] Daniel, Susan and a. M. K. Chaudhury, "Rectified motion of liquid drops on gradient surfaces induced by vibration," *Langmuir,* vol. 18, no. 9, pp. 3404-3407, 2002.

[36] Vasilev, K., Mierczynska, A., Hook, A.L., Chan, J., Voelcker, N.H. and Short,

R.D., "Creating gradients of two proteins by differential passive adsorption onto a PEG-density gradient," *Biomaterials,* vol. 31, no. 3, pp. 392-397, 2010.

[37] Kingshott, P., McArthur, S., Thissen, H., Castner, D.G. and Griesser, H.J., "Ultrasensitive probing of the protein resistance of PEG surfaces by secondary ion mass spectrometry," *Biomaterials,* vol. 23, no. 24, pp. 4775-4785, 2002.

[38] Snyders, R., Shingel, K.I., Zabeida, O., Roberge, C., Faure, M.P., Martinu, L. and Klemberg‐Sapieha, J.E., "Mechanical and microstructural properties of hybrid poly (ethylene glycol)–soy protein hydrogels for wound dressing applications," *Journal of Biomedical Materials Research Part A,* vol. 83, no. 1, pp. 88-97, 2007.

[39] Tripp, J.H., " Hertzian contact in two and three dimensions," *NASA Tech,* Paper 2473, July 1985.

[40] B. Amsden, "Solute diffusion within hydrogels. Mechanisms and models," *Macromolecules,* vol. 31, no. 23, pp. 8382-8395, 198.

[41] L. M. Weber, C. G. Lopez and K. S. Anseth, "Effects of PEG hydrogel crosslinking density on protein diffusion and encapsulated islet survival and function," *Journal of biomedical materials research Part A,* vol. 90, no. 3, pp. 720-729, 2009.

[42] K. Engberg and C. W. Frank, "Protein diffusion in photopolymerized poly (ethylene glycol) hydrogel networks," *Biomedical Materials,* vol. 6, no. 5, p. 055006, 2011.

[43] Lee, C.J., Vroom, J.A., Fishman, H.A. and Bent, S.F., "Determination of human lens capsule permeability and its feasibility as a replacement for Bruch's membrane," *Biomaterials,* vol. 27, no. 8, pp. 1670-1678, 2006.

[44] Y. Hiller, "Biotin binding to avidin. Oligosaccharide side chain not required for ligand association," *Biochemical journal,* vol. 248, no. 1, pp. 167-171, 1987.

Vita

Ruiqian Zhan was born in Changsha, Hunan, China. He received his B.S. degree in Mechanical Engineering from Optical and Electronical Information College of Changchun University of Science&Technology, Changchun, China. Then he came to the Department of Mechanical Engineering at the University of Kentucky for Master study.